NAVAL POSTGRADUATE SCHOOL
Monterey, California

THESIS

AN INVESTIGATION INTO THE FEASIBILITY OF USING A DUAL-COMBUSTION MODE RAMJET IN A HIGH MACH NUMBER TACTICAL MISSILE

by

Clifford B. Vaught

September 1987

Thesis Advisor: David W. Netzer

Approved for public release; distribution unlimited

UNCLASSIFIED
CURITY CLASSIFICATION OF THIS PAGE

REPORT DOCUMENTATION PAGE

REPORT SECURITY CLASSIFICATION UNCLASSIFIED	1b RESTRICTIVE MARKINGS
SECURITY CLASSIFICATION AUTHORITY	3 DISTRIBUTION/AVAILABILITY OF REPORT Approved for public release;
DECLASSIFICATION/DOWNGRADING SCHEDULE	distribution unlimited.
PERFORMING ORGANIZATION REPORT NUMBER(S)	5 MONITORING ORGANIZATION REPORT NUMBER(S)
NAME OF PERFORMING ORGANIZATION aval Postgraduate School	6b OFFICE SYMBOL (If applicable) 67
7a NAME OF MONITORING ORGANIZATION Naval Postgraduate School	
ADDRESS (City, State, and ZIP Code) onterey, California 93943-5000	7b ADDRESS (City, State, and ZIP Code) Monterey, California 93943-5000
NAME OF FUNDING/SPONSORING ORGANIZATION aval Weapons Center	8b OFFICE SYMBOL (If applicable)
9 PROCUREMENT INSTRUMENT IDENTIFICATION NUMBER	
ADDRESS (City, State, and ZIP Code) ina Lake, California 93555-6001	10 SOURCE OF FUNDING NUMBERS PROGRAM ELEMENT NO / PROJECT NO / TASK NO / WORK UNIT ACCESSION NO

TITLE (Include Security Classification)
N INVESTIGATION INTO THE FEASIBILITY OF USING A DUAL-COMBUSTION MODE RAMJET IN A HIGH ACH NUMBER TACTICAL MISSILE

PERSONAL AUTHOR(S)
aught, Clifford B.

TYPE OF REPORT	13b TIME COVERED	14 DATE OF REPORT (Year, Month, Day)	15 PAGE COUNT
aster's Thesis	FROM ___ TO ___	1987, September	84

SUPPLEMENTARY NOTATION

COSATI CODES			18 SUBJECT TERMS (Continue on reverse if necessary and identify by block number)
FIELD	GROUP	SUB-GROUP	Ramjet, scramjet, dual-combustion ramjet, supersonic combustion, solid fuel propulsion

ABSTRACT (Continue on reverse if necessary and identify by block number)

n investigation into the feasibility of using a solid fuel, dual combustion mode ram-et in a high Mach number tactical missile was conducted to determine the regimes where his propulsion plant might be superior to a conventional solid fuel ramjet. The results f the study show that at Mach 6, 80,000 feet, with a temperature rise combustion effi-iency of 90%, the DMRJ performance exceeded that of the SFRJ by 20% at near stoichio-etric overall fuel-to-air ratios, neglecting mixing losses in the supersonic combustor. t also appears that η_{AT} must be greater than 70% in order for the DMRJ to outperform he conventional SFRJ.

DISTRIBUTION/AVAILABILITY OF ABSTRACT ☒ UNCLASSIFIED/UNLIMITED ☐ SAME AS RPT ☐ DTIC USERS	21 ABSTRACT SECURITY CLASSIFICATION UNCLASSIFIED
NAME OF RESPONSIBLE INDIVIDUAL avid W. Netzer	22b TELEPHONE (Include Area Code) (408)646 - 2980 / 22c OFFICE SYMBOL 67Nt

FORM 1473, 84 MAR 83 APR edition may be used until exhausted
All other editions are obsolete

SECURITY CLASSIFICATION OF THIS PAGE
UNCLASSIFIED

Approved for public release; distribution is unlimited.

An Investigation into the Feasibility of Using a Dual-Combustion Mode Ramjet in a High Mach Number Tactical Missile

by

Clifford B. Vaught
Lieutenant, United States Navy
B.S., United States Naval Academy, 1980

Submitted in partial fulfillment of the requirements for the degree of

MASTER OF SCIENCE IN AERONAUTICAL ENGINEERING

from the

NAVAL POSTGRADUATE SCHOOL
September 1987

ABSTRACT

An investigation into the feasibility of using a solid fuel, dual combustion mode ramjet in a high Mach number tactical missile was conducted to determine the regimes where this propulsion plant might be superior to a conventional solid fuel ramjet. The results of the study show that at Mach 6, 80,000 feet, with a temperature rise combustion efficiency of 90%, the DMRJ performance exceeded that of the SFRJ by 20% at near stoichiometric overall fuel-to-air ratios, neglecting mixing losses in the supersonic combustor. It also appears that $\eta_{\Delta T}$ must be greater than 70% in order for the DMRJ to outperform the conventional SFRJ.

TABLE OF CONTENTS

LIST OF FIGURES

LIST OF SYMBOLS

A : area (in^2)
A/A^*: area ratio
C_D : coefficient of drag
C_p : specific heat (Btu/lbm-°R)
D : diameter (in)
F : thrust (lbf)
F/m_0: specific thrust (lbf-sec/lbm)
f : fuel-to-air ratio
G : mass flux (lbm/in^2-sec)
g_c : 32.174 ft-lbm/lbf-sec^2
h : altitude (ft)
J : 778 ft-lbf/Btu
L_g : grain length (in)
M : Mach number
m : mass flow rate (lbm/sec)
P : stagnation pressure (lbf/in^2)
p : static pressure (lbf/in^2)
R : gas constant (Btu/lbm-°R)
r : regression rate (in/sec)
S : specific fuel consumption (lbm/lbf-sec)
T : stagnation temperature (°R)
t : static temperature (°R)
u : velocity (ft/sec)
$\eta_{\Delta T}$: equilibrium adiabatic combustion efficiency
Φ : equivalence ratio
γ : ratio of specific heats
ρ : density (lbm/in^3)

ACKNOWLEDGEMENTS

I would like to offer my most sincere thanks and appreciation to Prof. Dave Netzer for giving me the opportunity to work with him on this project. His guidance and keen insight were the essential ingredients to this research effort. I would also like to thank Dr. Alon Gany for sharing with me his expertise in ramjet propulsion. Finally, I would like to thank the propulsion team of Mr. Pat Hickey, Mr. Don Harvey and Mr. Harry Connor for their time, talents and patience in constructing the dual-mode ramjet. Most of all, I would like to thank Netti, for her love and support, and for always helping me to keep things in perspective.

I. INTRODUCTION

The purpose of this study was to investigate the feasibility of utilizing a solid fuel, dual combustion mode ramjet (DMRJ) as the propulsion plant for a high Mach number tactical missile. As such, the primary objective was to examine the conditions under which the performance of a DMRJ might be superior to that of a conventional solid fuel ramjet (SFRJ) at a Mach number of 6.0 using realistic propulsion performance parameters. The secondary objective was to experimentally examine the feasibility of sustaining combustion in a Mach 2.5 flow.

There are many potential benefits from the development of a hypersonic vehicle. Among them are the nation's efforts to construct the aerospace plane for hypersonic travel through the upper and lower atmosphere for both civil aviation as well as space exploration. Benefits to the military include powerful tactical/strategic missiles and interceptor/fighter aircraft.

Past tactical missile designs have relied almost exclusively on solid rocket motors. Their simplicity of design, lightweight construction and ease of handling and storage makes them ideally suited for the environment aboard ships. Rockets have very high thrust-to-weight and can deliver reasonably high specific impulse. They are, however, limited to short ranges in order to have sufficient energy during the end-game of the intercept to

defeat defensive maneuvers by the target. The Navy's current suite of air-to-air missiles include the AIM-7M Sparrow, the AIM-9M Sidewinder and the AIM-54C Phoenix. All of these weapons have relatively short range with high thrust-to-weights, capable of attaining speeds on the order of Mach 1.5 to 2.5 above launch Mach.

With the advent of very long range detection radars, satellite targeting, over-the-horizon data link targeting and long range cruise missiles, these weapons are fast becoming incapable of adequately defending the fleet in a tactical scenario. New weapons like the Tomahawk and Harpoon cruise missiles utilize turbojet propulsion that has allowed greatly extended ranges. However they were designed for slow, non-maneuvering surface targets and are themselves subsonic. They are, therefore, practically useless against a tactical threat. What is needed is a long range, standoff weapon capable of reaching out 30 to 100 nautical miles with a high terminal velocity giving it sufficient energy to defeat the threat.

In order to achieve long ranges and high velocities, specifically terminal velocity, the vehicle must be powered throughout the full range of the flight. Rockets use boost and sustain propellant grains that burn out prior to intercept, generally leaving the missile to ultimately coast to the target. A pulsed motor is one means of extending the range of solid rockets. Another viable propulsion device for longer ranges is a high speed, airbreathing engine. Below Mach 2.5, the gas turbine

family of engines is inherently more efficient and will outperform all other air breathing power plants. At speeds greater than Mach 3.0, however, ram pressure alone is sufficient to provide proper compression of the airflow so that the compressor actually becomes a liability [Ref. 1: p. 38]. In addition, materials limit the maximum temperature allowed in the turbine section so that as Mach number increases, less and less energy can be added to the flow before that limit is reached. Thus, thrust falls off rapidly on the high speed end for a turbojet.

Between Mach 3.0 and 5.0, the ramjet becomes more efficient than the turbojet. Although ramjets have been around for some time, it has been only recently that their primary disadvantage has been overcome. Below Mach 0.9, ram pressure is insufficient to compress the flow adequately for efficient combustion [Ref. 2: p. 140]. Thus, a ramjet must be brought up to speed before it can be employed. The advent of the integral-rocket-ramjet (IRR) has made this possible, by employing a solid propellant booster to take the ramjet up to its take-over Mach number. Figure 1 presents the three power plants discussed thus far.

As the Mach number increases towards Mach 5.0, shock compression to subsonic velocities results in large losses in stagnation pressure. Here also, a temperature limit is reached for the combustion process due to dissociation of reactants in the flow. In addition, since subsonic combustion is most efficient when the incoming Mach number

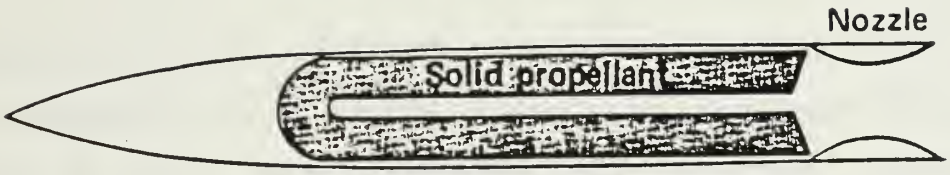

(a) Solid-fueled rocket

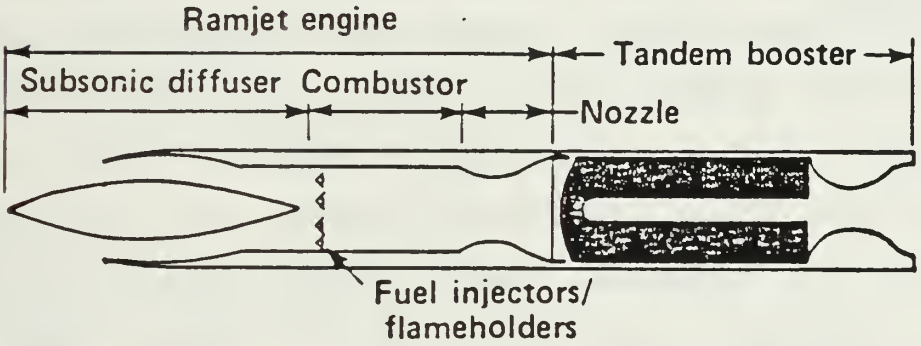

(b) Integral rocket ramjet

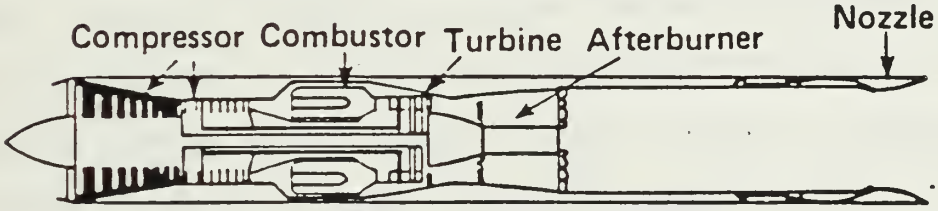

(c) Turbojet

Figure 1 - Propulsion systems for tactical missiles: (a) solid-fueled rocket; (b) integral rocket ramjet; (c) turbojet. [Adapted from Ref. 2: p. 139]

is on the order of 0.2 to 0.3, the static temperature and pressure in the combustor approach material limits. Figure 2 delineates the limits of the typical ramjet flight envelope.

In order to achieve hypersonic velocities, scramjet technology is the most feasible solution. The decrease in shock losses (reducing the combustor flow only to low supersonic velocities) more than offsets the increased heat addition losses from adding energy to a supersonic flow. The lower static temperature associated with supersonic flow ensures very little dissociation will occur and the need for cooling is reduced. This, in conjunction with lower pressures, reduces the structural limitation on the combustor itself. Thus, greater energy addition is possible, resulting in higher exhaust velocities and more thrust.

There are two types of scramjets. The first is a conventional ramjet with supersonic flow through the combustion chamber. This is accomplished by designing an inlet without a normal shock so that the flow remains supersonic. The second type of scramjet is more appropriately named a dual-combustion mode ramjet (DMRJ). This configuration involves using a conventional ramjet as a gas generator that exhausts into a second stream of supersonic bypass air. Mixing and combustion of the fuel-rich effluent occurs, enabling further heat release. Figure 3 illustrates both types of scramjets. The primary problem with the combustion process is whether or not sufficient

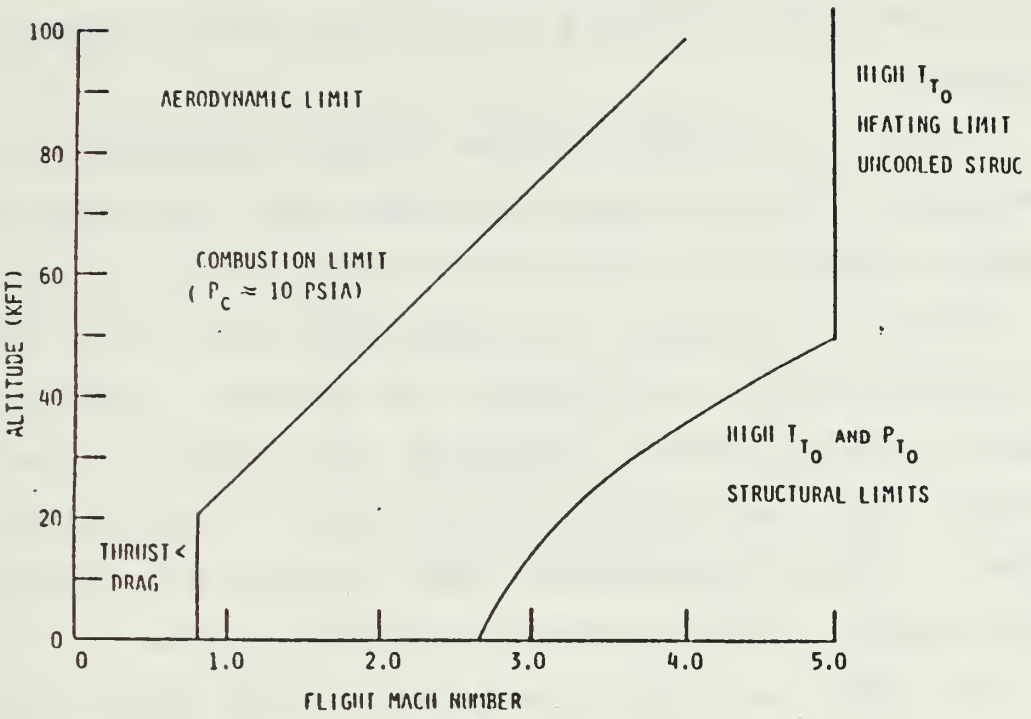

Figure 2 - Performance range of ramjets [Adapted from Ref. 3]

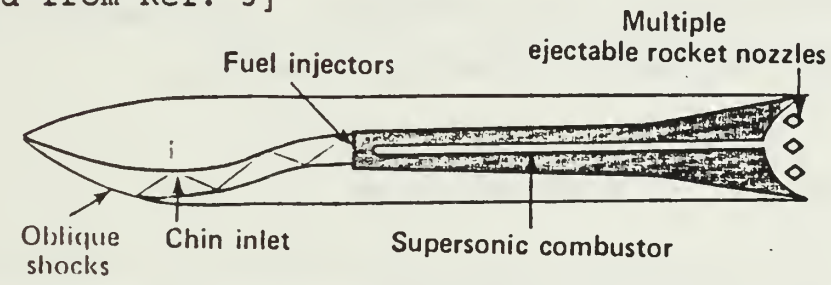

(a) Integral rocket liquid-fueled scramjet

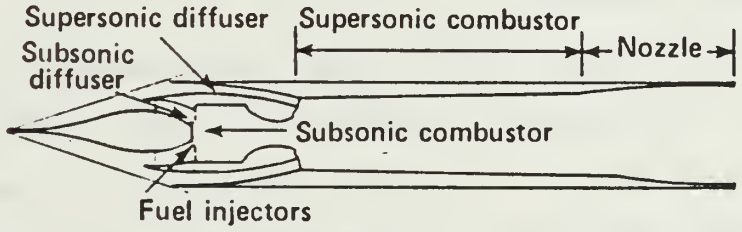

(b) Liquid-fueled dual-combustor ramjet.

Figure 3 - Supersonic combustion systems for tactical missiles. [Adapted from Ref. 2: p. 142]

residence time and mixing exist for sustained combustion, given the speed of the flow and the kinetic rates of the process.

Figure 4 illustrates the ideal performance of the propulsion devices discussed thus far, and the flight regimes in which they have advantages over each other.

There are several advantages associated with the use of solid fuels in both rockets and ramjets. Liquid fueled ramjets (LFRJ) require a positive fuel control, a means to atomize the fuel droplets and a means of stabilizing the flame. These requirements make the the LFRJ inherently more complex, as well as heavier, than the SFRJ.

The SFRJ is "self-throttling". The amount of mass flow taken into the engine and its properties determines the fuel flow rate in the combustor. The general expression for the regression rate for an SFRJ is:

$$\text{(eqn. 1)} \qquad r = \kappa\, G^x\, p^y\, t^z$$

where G represents the mass flux entering the combustor, p is the chamber pressure, t is the air inlet (static) temperature and x, y and z are specific to the fuel and generally lie between 0.1 and 0.8. The flame stabilization is accomplished through the geometry of the combustor rather than insertion of vee-gutters or other bluff body flameholders. Figure 5 illustrates the flow field in the flame stabilization region of an SFRJ combustor.

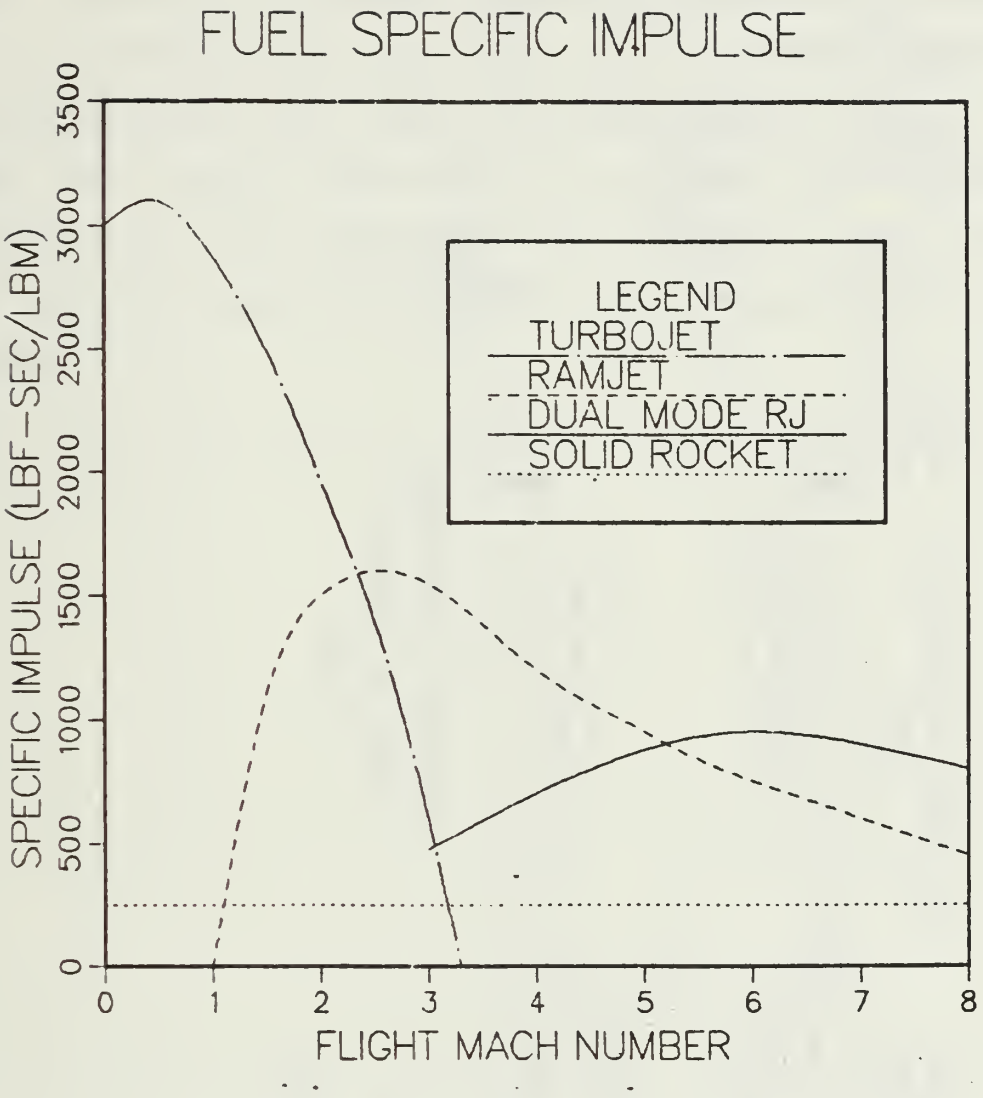

Figure 4 - Theoretical performance envelopes. [Adapted from Ref. 2: p. 144]

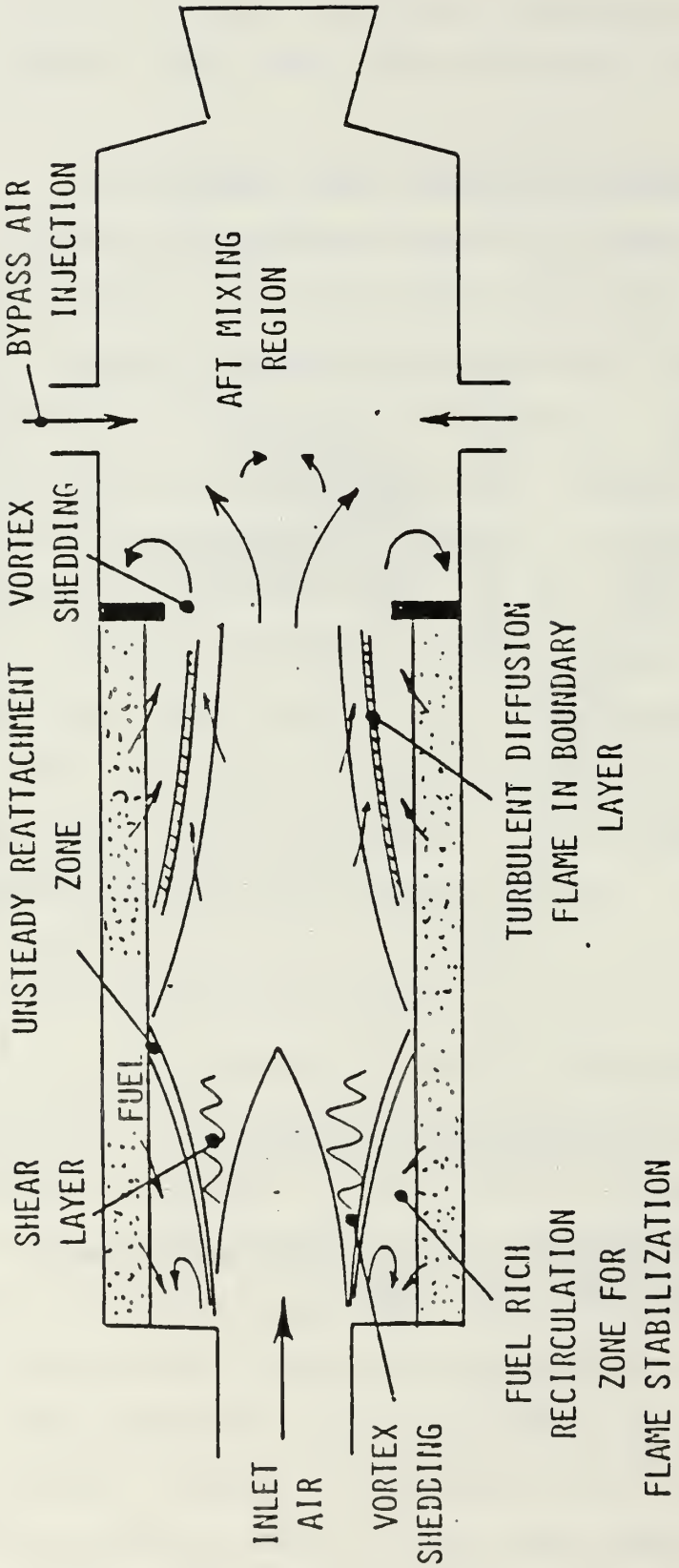

Figure 5 - Solid fuel ramjet engine [Ref. 4: p. 174]

Although the SFRJ is "self-throttling", the throttling is not optimum. The positive fuel controller in the LFRJ will enable it to achieve higher performance throughout the flight envelope than the SFRJ. This situation is changing as metallized fuels enable a higher energy density in the SFRJ fuel grain (resulting in improved performance) and variable air flow geometries are being developed. An SFRJ is able to achieve very high performance with a simple design.

II. NATURE OF THE PROBLEM

A. ANALYTICAL SOLUTION: SOLID FUEL RAMJET

For the purposes of this study, analytical models had to be assumed for both the SFRJ and the DMRJ. For the SFRJ the following conditions were employed:

(a) Design point: $M_0 = 6.0$; h = 80,000 ft; 1 lbm/sec flow rate

(b) Four-shock inlet with ramp angles of 12, 28 and 43 degrees (from horizontal), or an ideal inlet with no shock losses

(c) Inlet operating 10% supercritical

(d) Subsonic pressure recovery = 0.95 in the inlet

(e) Combustor inlet Mach = 0.2

(f) Constant area combustor

(g) One-dimensional flow in the combustor and nozzle

(h) HTPB grain as fuel (ρ = 0.0332 lbm/in^3)

(i) $C_D = 1.5$ in the SFRJ combustor

(j) Equilibrium, adiabatic combustion

(k) Nozzle throat choked

(l) Isentropic exhaust nozzle

(m) Frozen flow expansion through the exhaust nozzle to ambient pressure

Figure 6 depicts the station numbers in effect for the analysis.

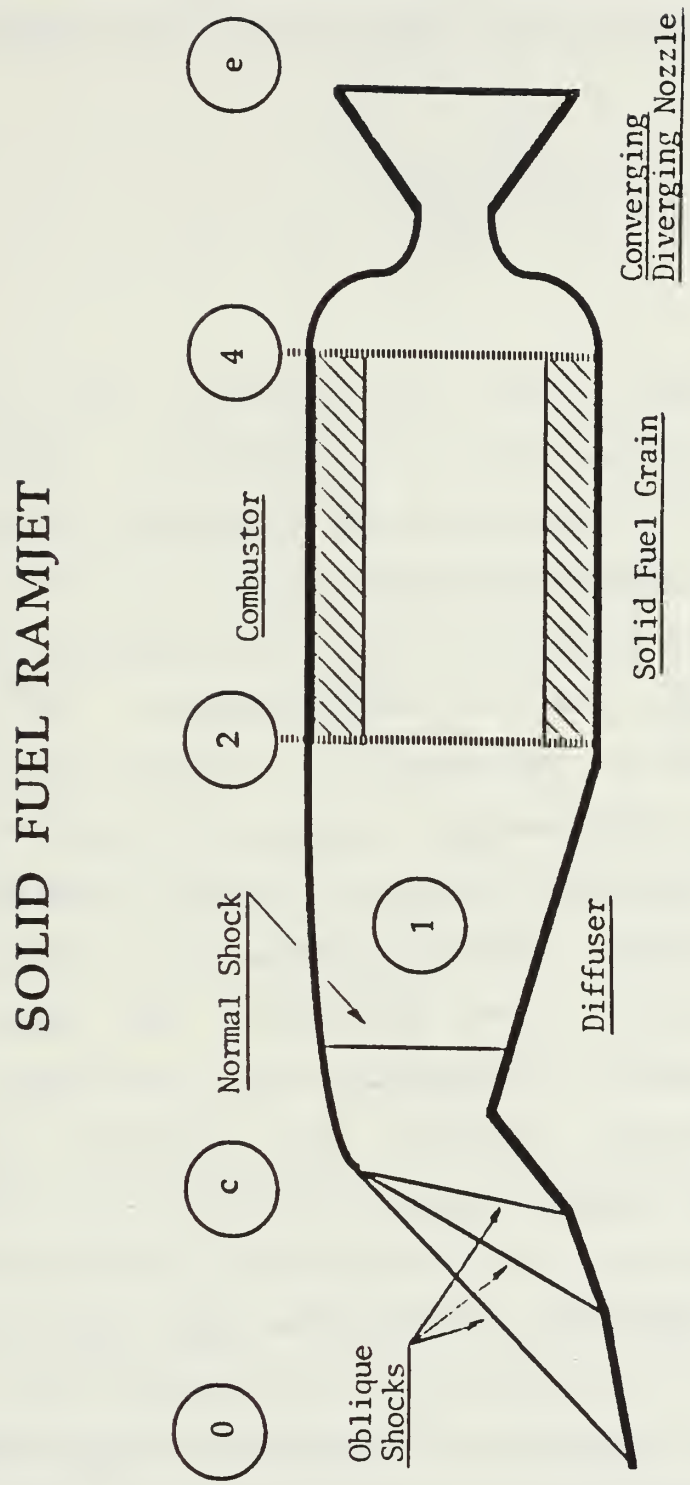

Figure 6 - Solid fuel ramjet model.

The continuity equation (conservation of mass), in the form below, was used to size the cowl and the combustor.

$$\text{(eqn. 2)} \qquad m = \frac{PA\sqrt{\frac{\gamma g_c}{RT}\left(\frac{2}{\gamma+1}\right)^{\frac{\gamma+1}{\gamma-1}}}}{A/A^*\Big|_M}$$

Oblique and normal shock relationships were used to determine the pressure loss up to station 2. With Mach number and flow rate specified and stagnation temperature known, equation 2 yields the area, A_2.

The only known parameters after the combustor were the throat Mach number and the exit pressure. To proceed across the combustor, conservation of energy and momentum are applied. For the energy equation, the Naval Weapons Center (NWC) Propellant Evaluation Program, PEPCODE, was used for equilibrium, adiabatic combustion to construct tables of combustion gas properties and theoretical stagnation temperatures at station 4 as a function of the stagnation properties entering the combustor and the fuel-to-air ratio (f) [Ref. 3]:

$$\text{(eqn. 3)} \qquad \text{PEPCODE} = \text{fn}(f,T,P) \Rightarrow T_{th},\ C_p,\ R,\ \gamma$$

Three tables are included in Appendix A. In order to determine the properties at station 4, knowing the properties from PEPCODE, the following equations had to be simultaneously satisfied to determine M_4:

(eqn. 4) $$\eta_{\Delta T} = \frac{T_4 - T_2}{T_{4th} - T_2}$$

(eqn. 5) $$\eta_{\Delta T} = \begin{cases} 1 - 0.35\Phi^{0.92} & \Phi \le 1 \\ 0.3 + 0.35\Phi^{0.92} & \Phi \ge 1 \end{cases}$$

where

(eqn. 5a) $$\Phi = \frac{f}{f_{stoich}}$$

(eqn. 6) $$T = t\left(1 + \frac{\gamma - 1}{2} M^2\right)$$

(eqn. 7) $$u = \sqrt{\gamma g_c R t}$$

(eqn. 8) $$p_i A_i - p_e A_e - F_D = m_e u_e - m_i u_i$$

(eqn. 8a) $$F_D = \frac{C_D p u^2}{2RTg_c}$$

(eqn. 9) $$P = p\left(1 + \frac{\gamma - 1}{2} M^2\right)^{\frac{\gamma}{\gamma - 1}}$$

RAMJET, an interactive computer code, was written to solve this system of equations, given the output of PEPCODE and an initial guess for M_4 as the input data. Each iteration was checked with the continuity equation until a specified tolerance was met. In this case, that tolerance was 0.0001 in mass flow rate. The exhaust velocity, thrust and specific fuel consumption (SFC) were then determined from:

(eqn. 10) $$u_e = \sqrt{2 C_p g_c J T_e \left[1 - \left(\frac{p_e}{P_e}\right)^{\frac{\gamma - 1}{\gamma}}\right]}$$

(eqn. 11) $$F = \frac{m_e u_e - m_0 u_0}{g_c}$$

(eqn. 12) $$SFC = \frac{m_f}{F}$$

A sample output is included in Appendix B, along with the program.

The grain length is determined by specifying Φ for each case. Equation 1 determined the regression rate with,

$$\begin{aligned} \kappa &= 7.1789\times10^{-5} \\ x &= 0.53 \\ y &= 0.33 \\ z &= 0.71 \end{aligned}$$

for HTPB. With fuel flow rate specified, the grain length, L_g, is determined from,

(eqn. 13) $$m_f = \rho_f \pi D_p L_g r$$

B. ANALYTICAL SOLUTION: DUAL COMBUSTION MODE RAMJET

As with the SFRJ, a model had to be created to determine all the properties through the DMRJ. In their 1958 paper on supersonic combustion, Weber and MacKay [Ref. 5] studied a one-dimensional model of a pure scramjet with a constant area combustor. Their model used liquid hydrogen as the fuel, for which a fixed combustion efficiency of 95% was assumed. They accounted for neither momentum losses

due to fuel injection in a high speed flow and shock losses in the combustor, nor were wall friction losses applied in the combustor. Dissociation was addressed briefly. For their study, the scramjet outperformed the conventional ramjet over the entire range of combustion temperatures examined (taken at an altitude of 120,000 ft. Mach 6) as long as there was no recombination in the exhaust nozzle expansion process (i.e., frozen flow) [Ref. 5: p. 106,110]. This stresses the impact on performance that dissociation has due to very high static temperature in the ramjet combustor. For an isentropic inlet, their scramjet model was superior to the conventional ramjet above Mach 7. With a wedge-type inlet, that advantage shifted to Mach 5. [Ref. 5: p. 102]

In this study, an attempt was made to take advantage of known realistic performance parameters for momentum loss in the SFRJ combustor and known subsonic combustion efficiency behavior of the solid fuel, HTPB. A one-dimensional, constant area combustor was also employed. Equilibrium adiabatic combustion through PEPCODE accounted for some of the effects of dissociation, though not completely, and yielded variable properties. Rather than assume a value of combustion efficiency, $\eta_{\Delta T}$ was used as a parameter in the performance study.

Figure 7 depicts a schematic representation of the DMRJ used in this study with applicable station numbers. Upstream of the "B" path of the mixer was an SFRJ gas generator identical to Figure 6. For use with the DMRJ,

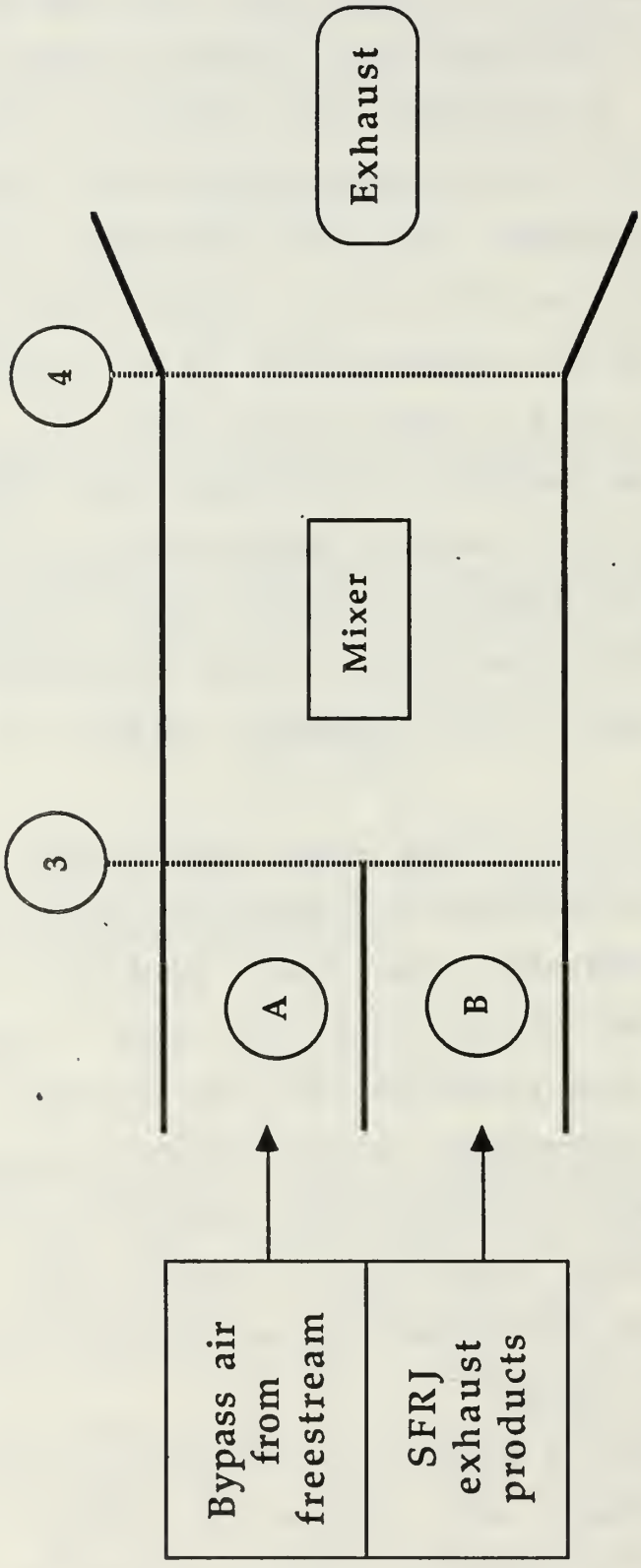

Figure 7 - Dual-mode ramjet mixer model.

however, station 4 has been renumbered as station 3. Two separate inlets were assumed; one for the SFRJ gas generator and one for bypass air. All the assumptions from the previous section for the SFRJ were applicable to the gas generator except in this case, the total design mass flow rate was 1 lbm/sec. For the bypass portion, the following conditions were employed:

(a) Three-oblique-shock inlet with the identical pressure recovery as the SFRJ inlet (prior to the normal shock), and an ideal inlet with no losses
(b) One-dimensional flow
(c) Mixer inlet Mach = 2.5
(d) Constant area supersonic mixer
(e) No mixing losses
(f) Static pressure at the mixer inlet determines exhaust pressure for the gas generator exhaust (i.e. SFRJ nozzle sized to match pressures at station 3)
(g) Equilibrium adiabatic combustion
(h) Frozen flow expansion to atmospheric conditions
(i) Isentropic nozzle

The method for solving the SFRJ portion of the DMRJ was identical to the previous section, except that the exhaust pressure was now equal to p_{3A}, vice atmospheric. RAMJET was again used to determine all the properties at station 3B. As before, oblique shock relationships were used to determine the properties at station 3A. Equation 2 was then used to determine the areas at stations 3A and 3B.

The mixing process presented the most difficulty in the analysis. No information was available in the open literature to make a reasonable assumption for the mixing loss. The approach taken was to assume a value of thermal efficiency ($\eta_{\Delta T}$), representing losses in the heat release process only, to vary the equivalence and bypass ratios and to not account for the mixing loss at all. From this, a "baseline" performance could be identified to which mixing losses could be applied as they become known.

PEPCODE was again employed to determine the properties at the exit of the mixing chamber, given the stagnation temperature of the Mach 6.0 flow, an estimate of the chamber stagnation pressure (to be verified) and the fuel-to-air ratio (f). In this analysis, a mass averaged temperature was determined for station 3, assuming complete mixing and no combustion, defined as:

(eqn. 14)
$$\overline{T_3} = \frac{m_{3A}C_{p3A}T_{3A} + m_{3B}C_{p3B}T_{3B}}{(m_{3A} + m_{3B})\overline{C_{p3}}}$$

Proceeding as before, with eta specified arbitrarily, all the properties known at station 3, and station 4 gas properties from PEPCODE, all the flow properties at station 4 were determined by solving equations 2,4,6,7 and 9 simultaneously.

MIXER, another interactive code, was written to solve this simultaneous set. Input variables included all the properties at stations 3A and 3B, the PEPCODE output for station 4 and an estimate of the Mach number at station 4.

Rather than using the continuity equation as the check, this program determines the velocity of the flow at station 4 by two means: (1) by equations 4,6 and 7; (2) by conservation of momentum, equation 8. Repeated estimates of the Mach number are made until the difference between the two velocities were on the order of 0.1% . This program and a sample output are included as Appendix C.

Once the properties at station 4 were determined, the exhaust velocity, thrust and specific fuel consumption were again determined using equations 10 - 12. This calculation was performed for each bypass ratio considered and each value of thermal efficiency.

III. ANALYTICAL RESULTS

A. SOLID FUEL RAMJET

The performance of the SFRJ is shown in Figure 8. The cases considered were: 1) design Mach number of 6.0, 4-shock inlet; 2) design Mach number of 6.0, isentropic inlet; and 3) design Mach number of 4.0, 4-shock inlet. All cases were done for an altitude of 80,000 feet. Tables of properties for these engines are included in Appendix D.

The shape of the curves is highly dependent on the adiabatic combustion efficiency, $\eta_{\Delta T}$. Figure 9 represents a plot of equation 5, which is the efficiency behavior of HTPB. The minimum at $\Phi = 1.0$ explains the pronounced dip in the performance curve. This dip is present with or without losses, regardless of design Mach number. The lower design Mach number, however, is more sensitive to changes in $\eta_{\Delta T}$. For example, for an overall equivalence ratio of 1.3 ($\eta_{\Delta T} \approx 0.75$), a 1% change in efficiency at Mach 4 will cause a 37% greater temperature rise than for Mach 6:

$$\eta_{\Delta T} = \frac{\Delta T}{\Delta T_{th}} = \frac{2243}{3011}\Big|_4 = \frac{1640}{2200}\Big|_6$$

This temperature rise is directly related to the exhaust velocity, therefore the thrust. Thus, trends in the performance curve are accentuated at the lower Mach number.

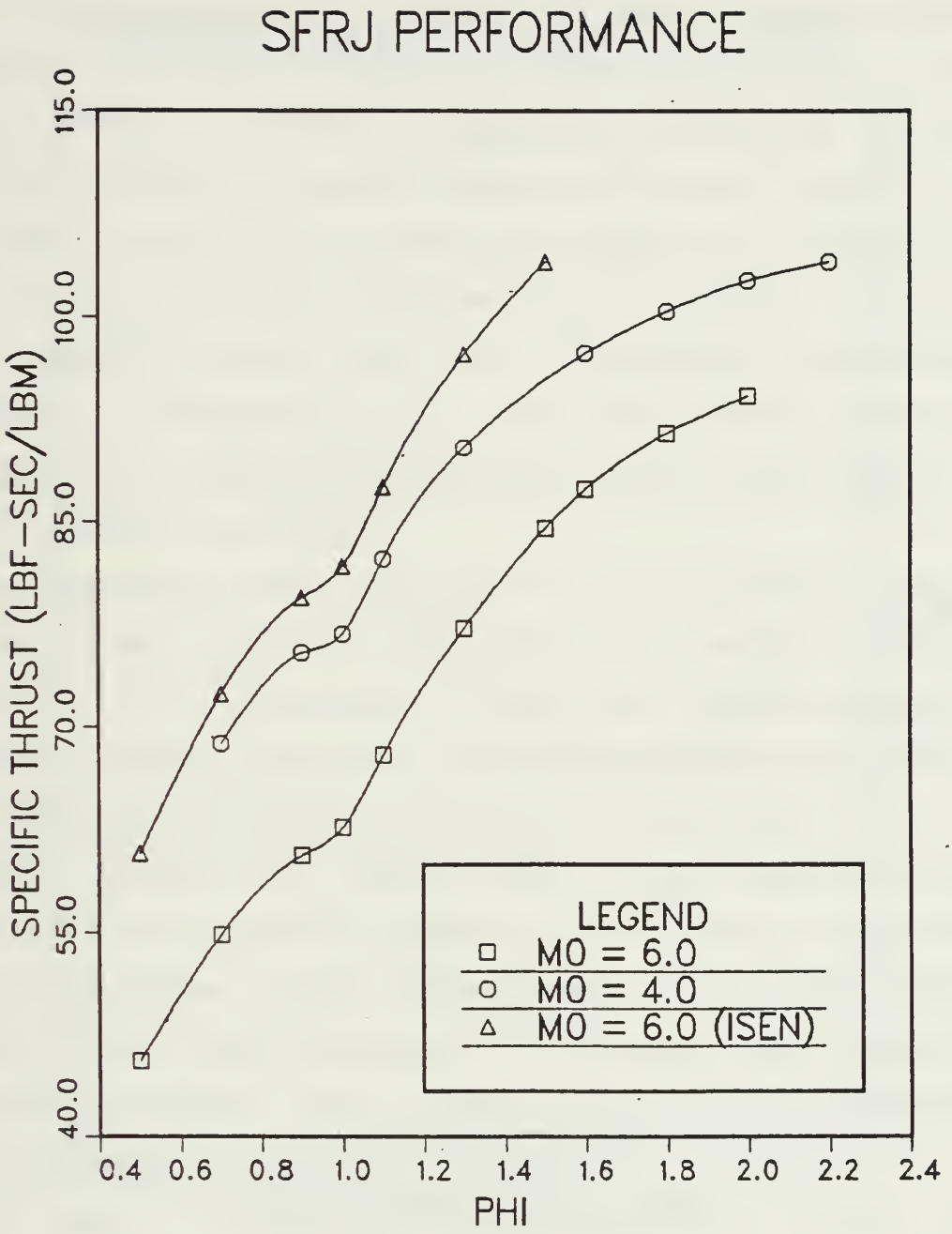

Figure 8 - Solid Fueled Ramjet performance for design altitude of 80,000 ft.

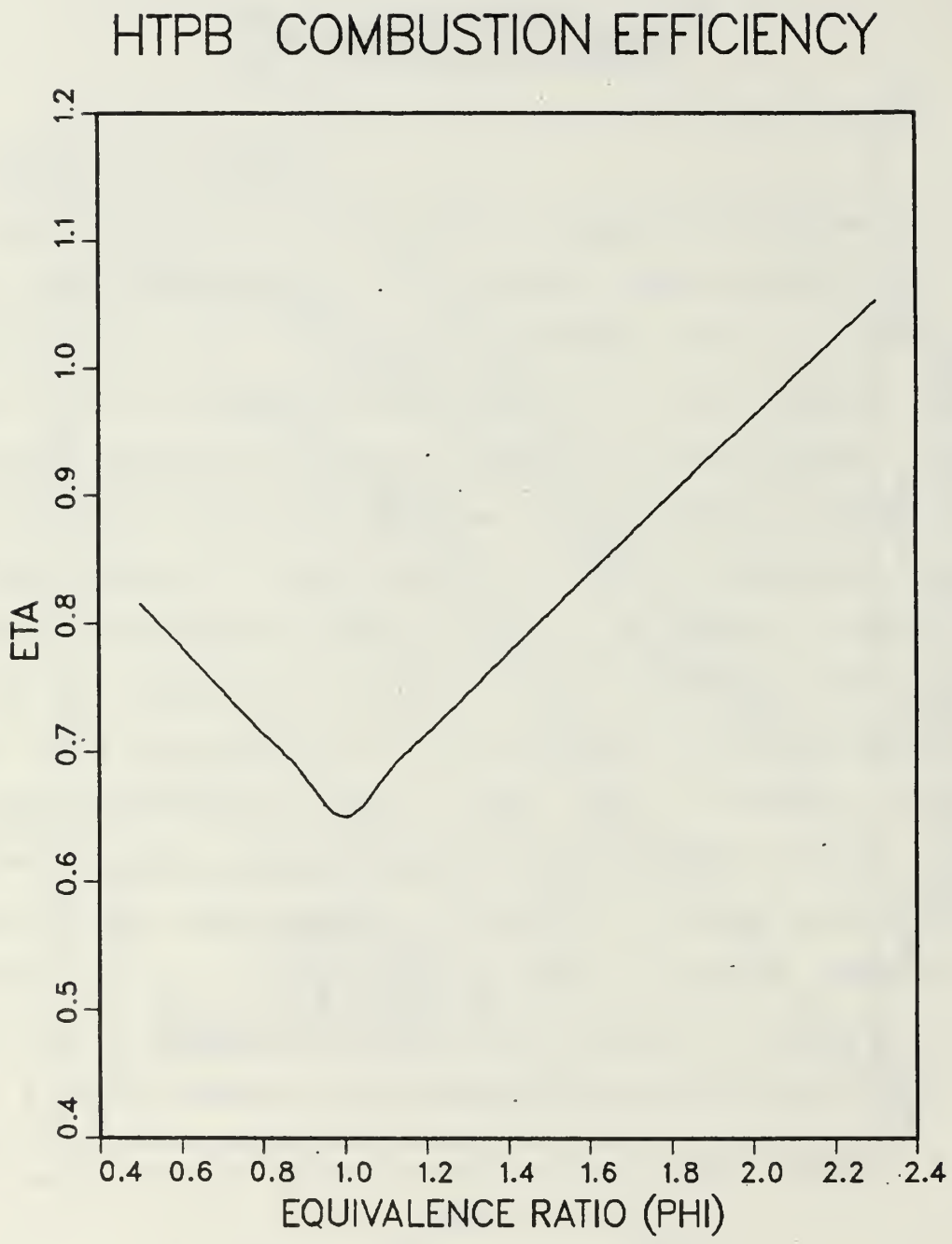

Figure 9 - Equilibrium adiabatic combustion efficiency for HTPB.

The performance curves indicate that specific thrust rises with Φ despite the behavior of T_{4th}, which is shown in Figure 10. The reason for this is two-fold. The primary effect is that of decreasing molecular weight. This is reflected in higher values of the gas constant, R, for higher values of Φ (refer to tables in Appendix A). Equation 10 shows that the dependence of exhaust velocity, and therefore, thrust, is $\sqrt{R}$. In addition, increasing Φ implies an increase in m_e. Thus, both of the terms in the jet thrust ($m_e u_e$) increase while the ram drag term ($m_0 u_0$) remains constant.

The secondary effect is that of the increasing combustion efficiency of HTPB in the fuel-rich regime (refer to Figure 9). The combination of these two effects appear to offset the sharp decrease in theoretical adiabatic combustion temperature, enabling the thrust to increase.

Inlet losses also have a very large effect on the performance of the SFRJ. Figure 8 shows that for the same design Mach number, inlet losses reduce the specific thrust of the SFRJ by approximately 20% throughout the range of equivalence ratios. This is due solely to the stagnation pressure drop across the inlet system.

The Mach 4 curve lies above the Mach 6 curve, as expected for a ramjet. The ram drag is the primary reason for this, as illustrated below for $\Phi = 1.8$.

M_0	u_e	T_4	F	u_0
6.0	7728	4850	91.5	5806
4.0	6272	3813	100.4	3872

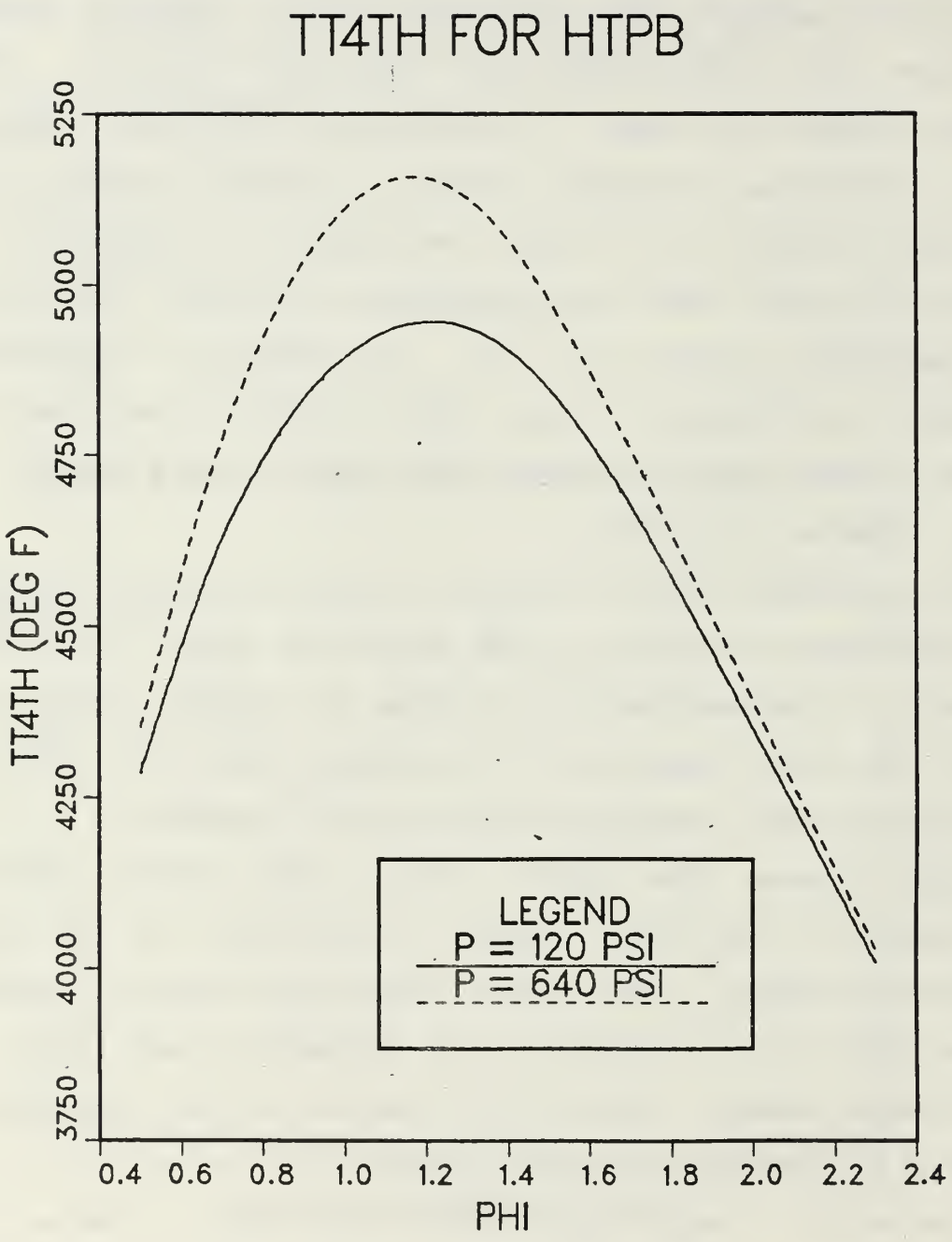

Figure 10 - Equilibrium adiabatic combustion temperature for HTPB for isentropic inlet (640 psi) and for 4-shock inlet (120 psi).

Although there is a large increase in exhaust velocity in going to Mach 6, there is an even greater increase in the freestream velocity, which leads to higher thrust at Mach 4.

A second contributor to the higher performance at the lower Mach number is the decrease in shock losses due to the weaker shocks at Mach 4.

Dissociation effects are accounted for by PEPCODE. As expected for the SFRJ, an increase in design Mach number diminishes the effect of adding fuel to the flow. For example, for $M_0 = 2.8$, the difference in theoretical stagnation temperature rise across the combustor going from $\Phi = 0.5$ to $\Phi = 1.0$ (i.e., doubling the fuel flow) is approximately 1300°R. For $M_0 = 6.0$, however, the same increase in fuel flow leads to a difference in theoretical stagnation temperature of approximately 580°R. This is the effect of dissociation on energy addition potential.

The unique combustion efficiency behavior for the SFRJ results in a predicted F/m_0 versus Φ behavior that is somewhat different than the behavior that is usually reported for ramjets with fixed combustion efficiency. Specific thrust will maximize at very rich equivalence ratios.

B. DUAL-MODE RAMJET

The results from the analytical model support the previous theoretical works of both Billig [Ref. 2] and Weber & MacKay [Ref. 5]. The performance of the DMRJ

exceeds the performance of the conventional SFRJ, within the constraints of the conditions applied, by approximately 20% in the range of anticipated equivalence ratios (0.8 - 1.1). Each parameter was examined for its impact on the calculations and results. However, because no attempt was made to account for mixing/shock/wall friction losses in the supersonic combustor, these results identify a minimum required performance, or a "baseline", to which these losses must be applied.

The parameters examined included the combustion efficiency ($\eta_{\Delta T}$), the bypass ratio[1], the design Mach number and the overall equivalence ratio. The effects of using an isentropic inlet were looked at briefly, as well as the impact of dissociation in the supersonic combustor. The following bypass ratios were used in the analysis: 50/50 (i.e., 50% primary air, 50% bypass air), 60/40, 75/25 and 80/20. Tables of properties through the engines are included in Appendix E and will be referred to below.

It must be emphasized that each point represents a different design condition and, therefore, a different engine. Each engine was re-sized as a parameter was changed and then flown at its design point. (The design point was Mach 6, 80,000 feet unless otherwise specified.)

1. Performance Comparison: $\eta_{\Delta T}$

As with the SFRJ, the performance of the DMRJ is highly sensitive to the combustion efficiency specified.

[1] Bypass ratio is defined as the ratio of mass flow through the primary gas generator to the mass flow through the bypass duct.

The gas generator has the same efficiency characteristics as the SFRJ (refer to Figure 9). The efficiency in the supersonic combustor was varied between 0.25 and 0.9.

Figure 11 is a plot of specific thrust versus the overall equivalence ratio for the conventional SFRJ, the DMRJ with an efficiency of 90% for all bypass ratios and the DMRJ for a combustion efficiency of 25% for two bracketing bypass ratios.

To understand the effect that efficiencies have on the DMRJ, it was necessary to compare an isentropic SFRJ to an isentropic DMRJ with $\eta_{\Delta T} = 1.0$ for all combustion processes. In this case, the engines were isentropic in that there were no inlet losses present. For the table below, $M_0 = 6.0$, h = 80,000 ft. and $\Phi_{TOT} = 1.0$ (i.e., same total fuel flow).

	SFRJ	80/20	50/50
Φ_{SFRJ}	1.00	1.25	2.00
T_3	--	5600	4848
T_4	5565	5565	5565
P_4	593	445	291
M_4	0.33	2.10	1.48
$\lvert P_4-P_0 \rvert$	45	193	347
T_{3ave}	--	5230	4166
ΔT	--	335	1399
t_4	5490	3544	4355
F/m_0	103.6	101.4	97.4

What this information shows is that at Mach 6, 80,000 ft., the SFRJ has superior performance to the DMRJ. The reason behind this is the stagnation pressure drop due just to heat addition. For the SFRJ with subsonic heat addition, the drop is very small. It, therefore has the

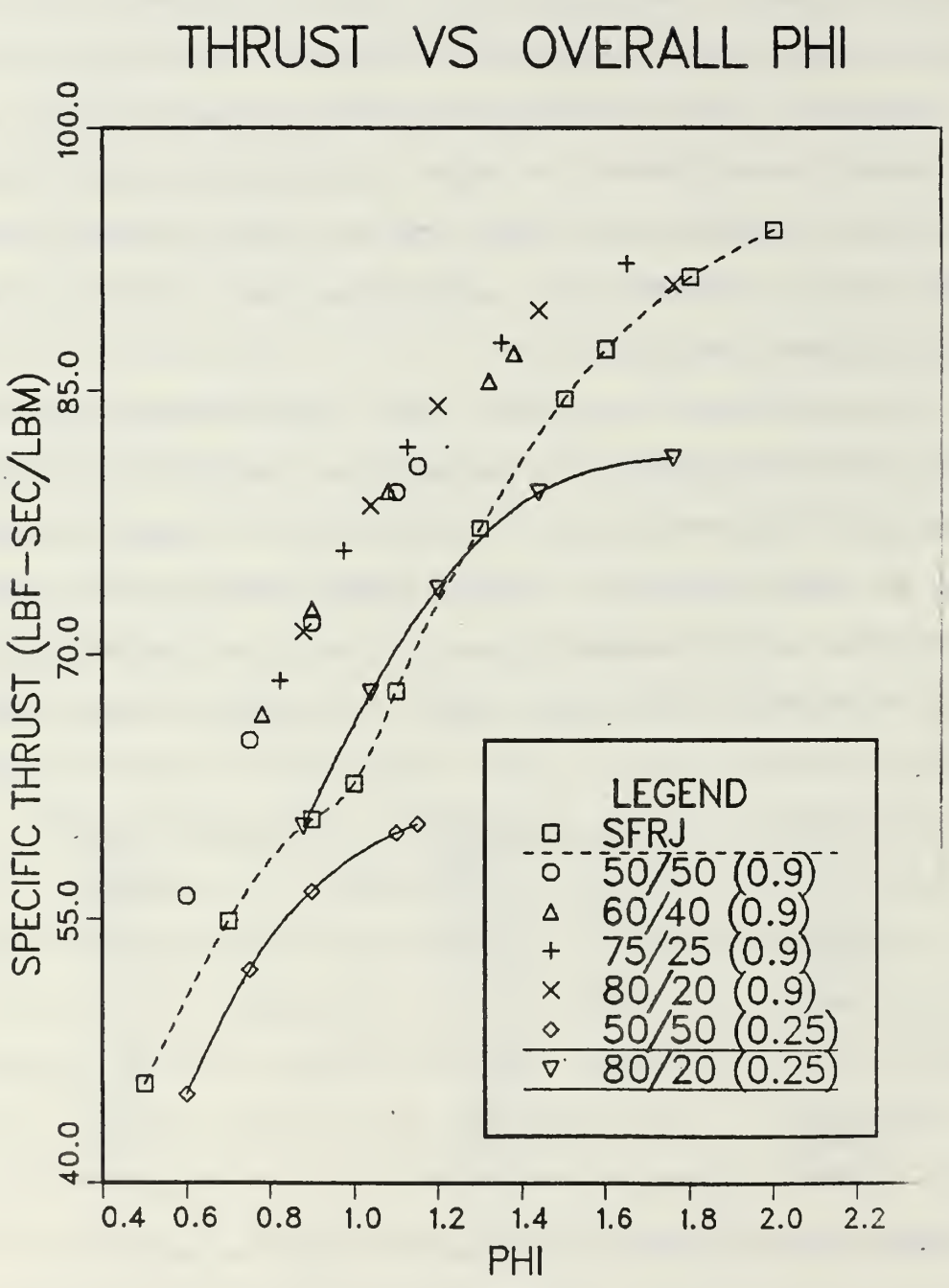

Figure 11 - Performance comparison for SFRJ, DMRJ with $\eta_{\Delta T}$ = 0.9 for four bypass ratios and DMRJ with $\eta_{\Delta T}$ = 0.25 for two bracketing bypass ratios. (M_0 = 6.0, 80,000 feet)

highest stagnation pressure. For the 50/50 DMRJ, the cooling effect of the bypass air is very significant (T_{3ave} = 4166°R). With considerable unburned fuel and a low inlet temperature, much of the heat addition occurs in the supersonic flow. Thus, it has the largest pressure drop. The 80/20 DMRJ lies between these two extremes. This result supports the finding of Weber & MacKay that for the same heat addition (both types of engines have the same T_4) the engine with the highest P_4 will have the highest exhaust velocity, which means highest thrust [Ref. 5: p. 104].

$\eta_{\Delta T}$ will affect the stagnation temperature at the exit of the combustor, supersonic or subsonic. When $\eta_{\Delta T}$ = 0.9 in the supersonic flow, the DMRJ exhibits a signifigant performance advantage at lower values of overall equivalence ratio. However, on the fuel-rich end, the DMRJ levels off while the SFRJ continues to increase, eventually causing a cross-over in performance. This behavior is explained in the table below for a DMRJ with a bypass ratio of 80/20:

	DMRJ	SFRJ		DMRJ	SFRJ
Φ_{SFRJ}	1.10	0.90		2.20	1.80
Φ_{TOT}	0.88	0.90		1.76	1.80
T_{3Bth}	5391	5292		4581	5031
T_{3B}	4693	4626		4612	4850
T_4	5195	4626		5008	4850
F/m_0	71.3	60.6		91.1	91.5
$\eta_{\Delta T}$:RJ	0.68	0.68		1.02	0.90
$\eta_{\Delta T}$:DJ	0.90	--		0.90	--

The first two columns represent a comparison at the fuel-lean end ($\Phi_{TOT} \approx 0.9$) where the DMRJ has a distinct

performance advantage. The third and fourth columns compare the SFRJ and DMRJ at the fuel-rich end ($\Phi_{TOT} \approx 1.8$) where the performance crosses over.

For the first case, the SFRJ efficiencies are identical so that the temperature at the exit of the combustors are nearly the same. The only difference was that $\Phi = 1.1$ lies closer to the peak of the temperature profile, shown in Figure 10, than does $\Phi = 0.9$, leading to a higher theoretical stagnation temperature, hence a higher actual stagnation temperature. T_4 is then significantly higher due to very efficient burning of the excess fuel in the second combustion process. This is the driver behind the performance advantage for the DMRJ at the lean end of overall equivalence ratio.

For the second case, the performance is very nearly equal, with the SFRJ being slightly superior. In this case, the DMRJ primary combustor is very fuel rich at a Φ of 2.2. This point is well past the peak in theoretical stagnation temperature for HTPB. The DMRJ actually exhibits a drop in stagnation temperature at the primary burner exit from an increase in the fuel flow while the SFRJ exit temperature increases. The efficiency behavior of HTPB causes the actual exit temperature to increase slightly, but it is still less than the exit temperature for the SFRJ. The crossover in performance for the SFRJ comes from a combination of higher stagnation pressure and smaller molecular weight (larger R) that just offsets the difference in T_4.

Figure 12 is a plot of DMRJ specific thrust versus overall Φ for two bypass ratios with $\eta_{\Delta T}$ as a parameter. This plot shows the increment by which the performance varies with efficiency. It appears that for any realistic advantage from the dual-mode to exist, combustion efficiencies on the order of 70% should be attained (refer to Figures 11 & 12). In the general region of interest (i.e., $\Phi < 1.2$), 50% efficiency leads to near equal performance to the SFRJ accounting for heat addition losses but no mixing or shock losses.

2. Performance Comparison: Bypass Ratio

Both Figure 11 and 12 demonstrate the dramatic effect of decreasing bypass ratio as efficiency decreases. For very high supersonic combustion efficiency, the performance lines for each bypass ratio very nearly overlay. However, as that efficiency is decreased, the performance lines begin to diverge. For the same value of overall Φ, there is a large difference in performance between a bypass ratio of 80/20 and one of 50/50. In the table below, a closer examination is made for $M_0 = 6.0$, 80,000 ft. with inlet losses and with $\eta_{\Delta T} = 0.5$:

	50/50	80/20
Φ_{TOT}	0.90	0.88
Φ_{SFRJ}	1.80	1.10
$\eta_{\Delta T}$ |RJ	0.90	0.68
m_f	0.066	0.065
T_{3th}	5031	5391
T_3	4850	4693
T_{3ave}	4193	4463
T_4	4743	4871
F/m_0	62.6	64.5

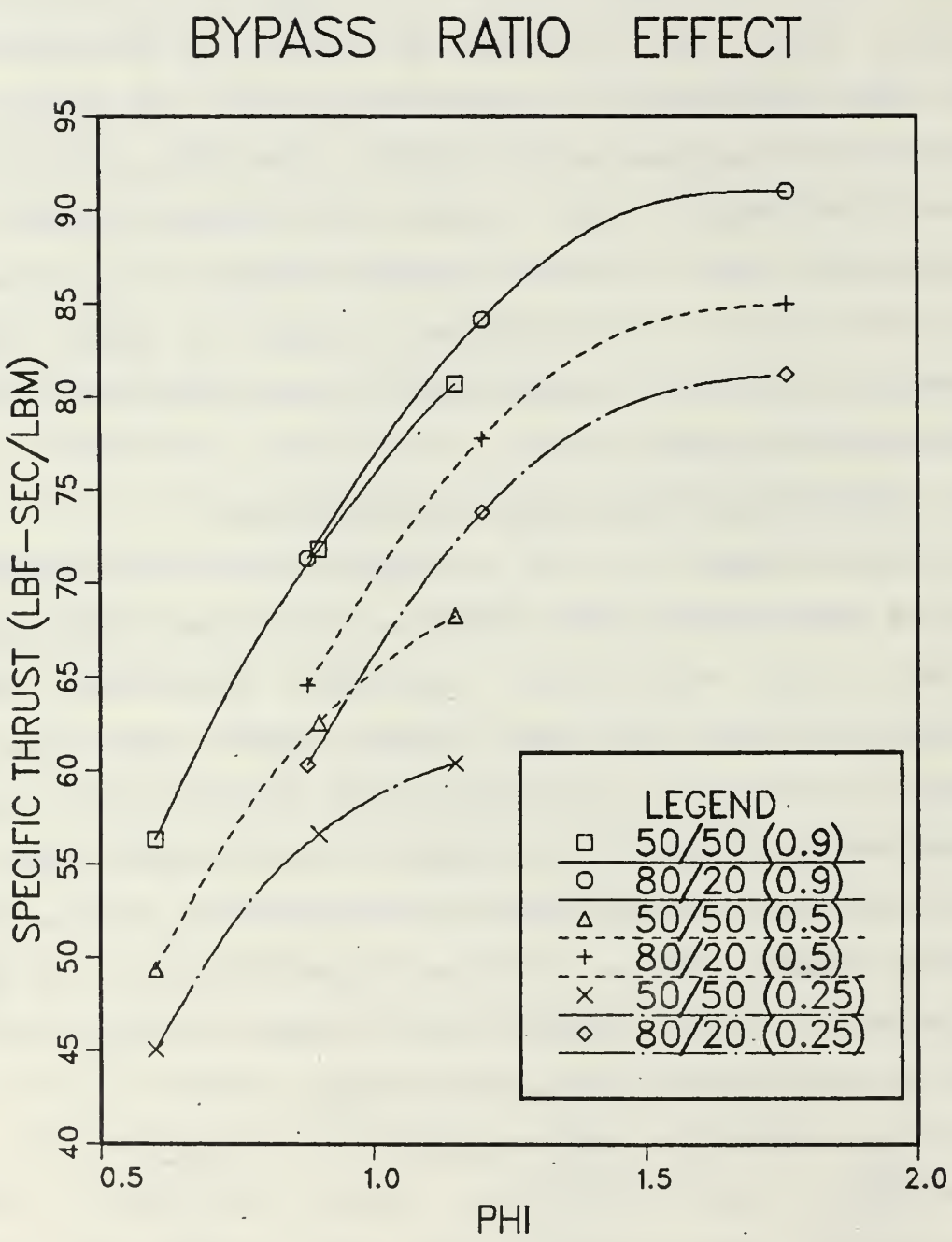

Figure 12 - Effect of $\eta_{\Delta T}$ on two bypass ratios. (M_0 = 6.0, 80,000 ft., with inlet losses)

For very nearly the same fuel flow, there is a difference in performance. Even though the 50/50 DMRJ has a higher stagnation temperature exhausting into the mixer (T_3), due to the higher $\eta_{\Delta T}$, T_{3ave} is significantly lower due to the larger amount of cooler bypass air (T_0 = 3198). This causes T_4 for the 50/50 DMRJ to be lower than the 80/20 DMRJ, leading to a higher specific thrust for the larger bypass ratio for nearly the same amount of fuel addition.

Another effect of bypass ratio is that to obtain high values of overall Φ, larger bypass ratios must be used. For example, to obtain an overall equivalence ratio of 1.5 would require Φ_{SFRJ} = 1.875 for the 80/20 DMRJ. The 50/50 DMRJ however, would require a primary combustor equivalence ratio of 3.0, for which the efficiency data for HTPB is not applicable. Thus, for any specified overall equivalence ratio, the 50/50 DMRJ will be much more fuel-rich than the 80/20 DMRJ.

One final observation is that although the combustion efficiency in the primary combustor is higher in terms of temperature rise for the fuel-rich engines (lower bypass ratios), there will be more unburned fuel present in the supersonic combustor. For a high $\eta_{\Delta T}$ in the supersonic combustor, it doesn't appear to matter, and the performance of the two cases should be similar. Figure 12 verifies this behavior. For the lower $\eta_{\Delta T}$ in the supersonic combustor, that excess fuel is burned less efficiently so that a

performance difference should exist. This behavior is also depicted in Figure 12.

3. Performance Comparison: M_0

Figure 13 shows how decreasing the design Mach number to Mach 4 (80,000 ft.) affects the performance of the SFRJ and the DMRJ. The bypass ratio of the DMRJ is 80/20 and the combustion efficiency is 90%. Inlet losses are included. As in the case of the SFRJ, going to a lower Mach number improves the performance of the DMRJ for the same reasons: lower shock losses and reduced ram drag. Figure 14 includes an 80/20 DMRJ with $\eta_{\Delta T} = 0.6$ to show the effect of changing the efficiency and the Mach number.

4. Performance Comparison: Inlet losses

The effect of using an isentropic inlet on the DMRJ with $\eta_{\Delta T} = 0.9$ is depicted in Figure 15. Just as the performance for the SFRJ increases, the DMRJ realizes a gain in specific thrust of approximately 25% at Mach 6, 80,000 ft. The reason for the improvement, as before, is the absence of stagnation pressure losses due to inlet shocks. The SFRJ is included in Figure 15 to show that the isentropic DMRJ gives the best performance.

5. Performance Comparison: Dissociation

One of the reasons for going to supersonic combustion over subsonic is dissociation of the reactant molecules due to the extremely high static temperatures that are encountered when a high speed flow is shocked down to low subsonic Mach numbers (0.15 to 0.3). Dissociation

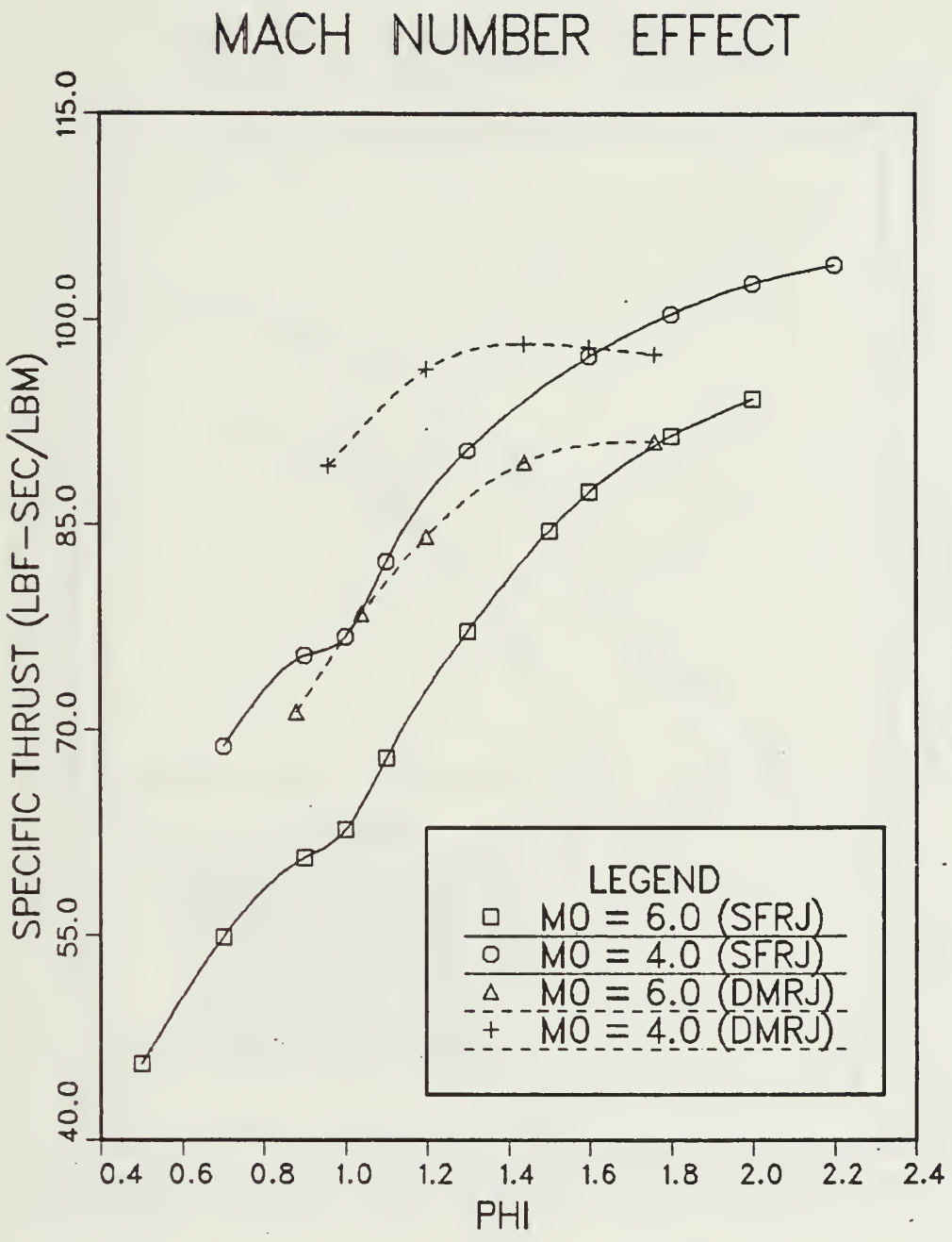

Figure 13 - Effect of design Mach number on performance for SFRJ and 80/20 DMRJ with $\eta_{\Delta T}$ = 0.90. (4-shock inlet, 80,000 ft.)

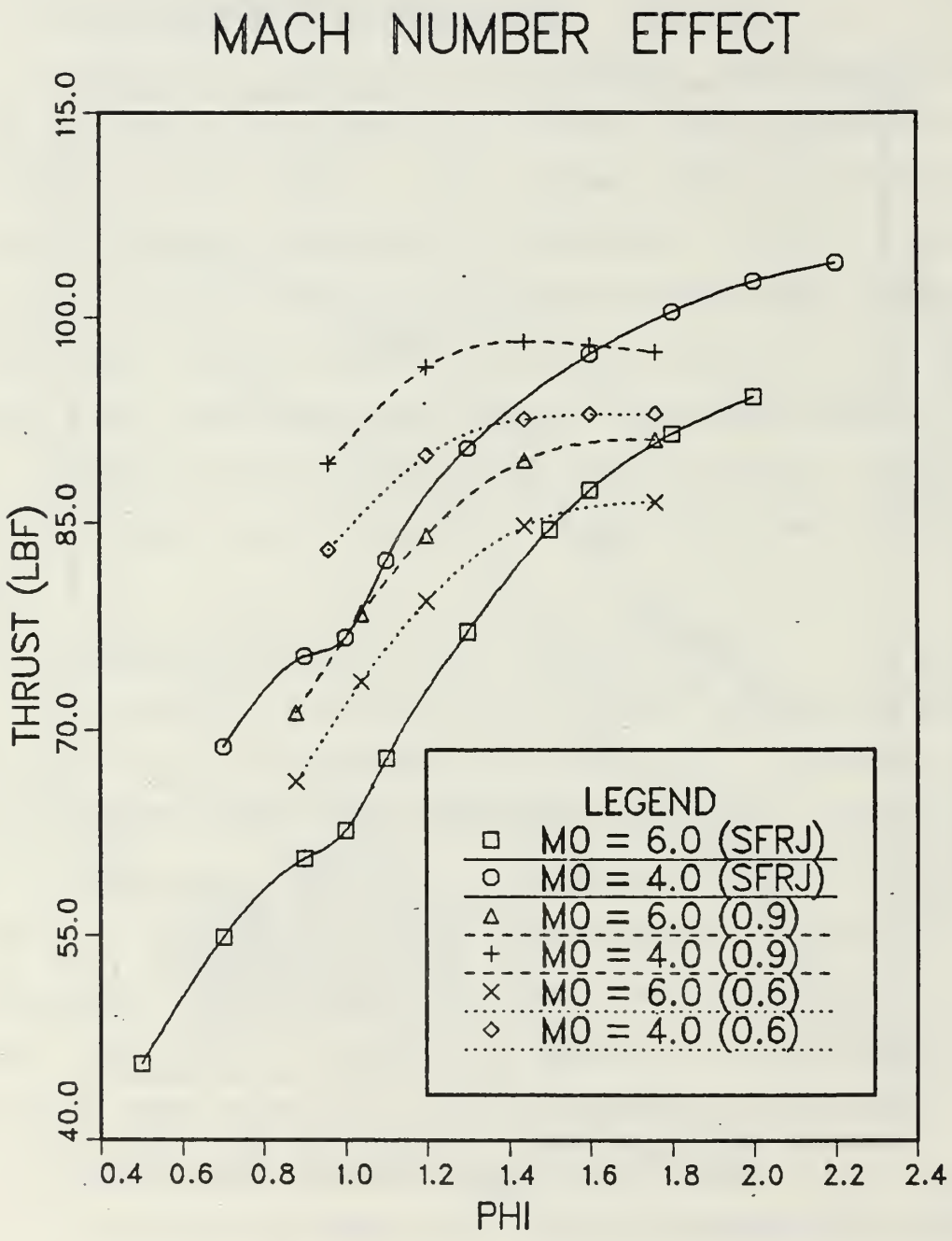

Figure 14 - Effect of design Mach number for SFRJ and 80/20 DMRJ for two values of $\eta_{\Delta T}$, 0.60 and 0.90. (4-shock inlet, 80,000 ft.)

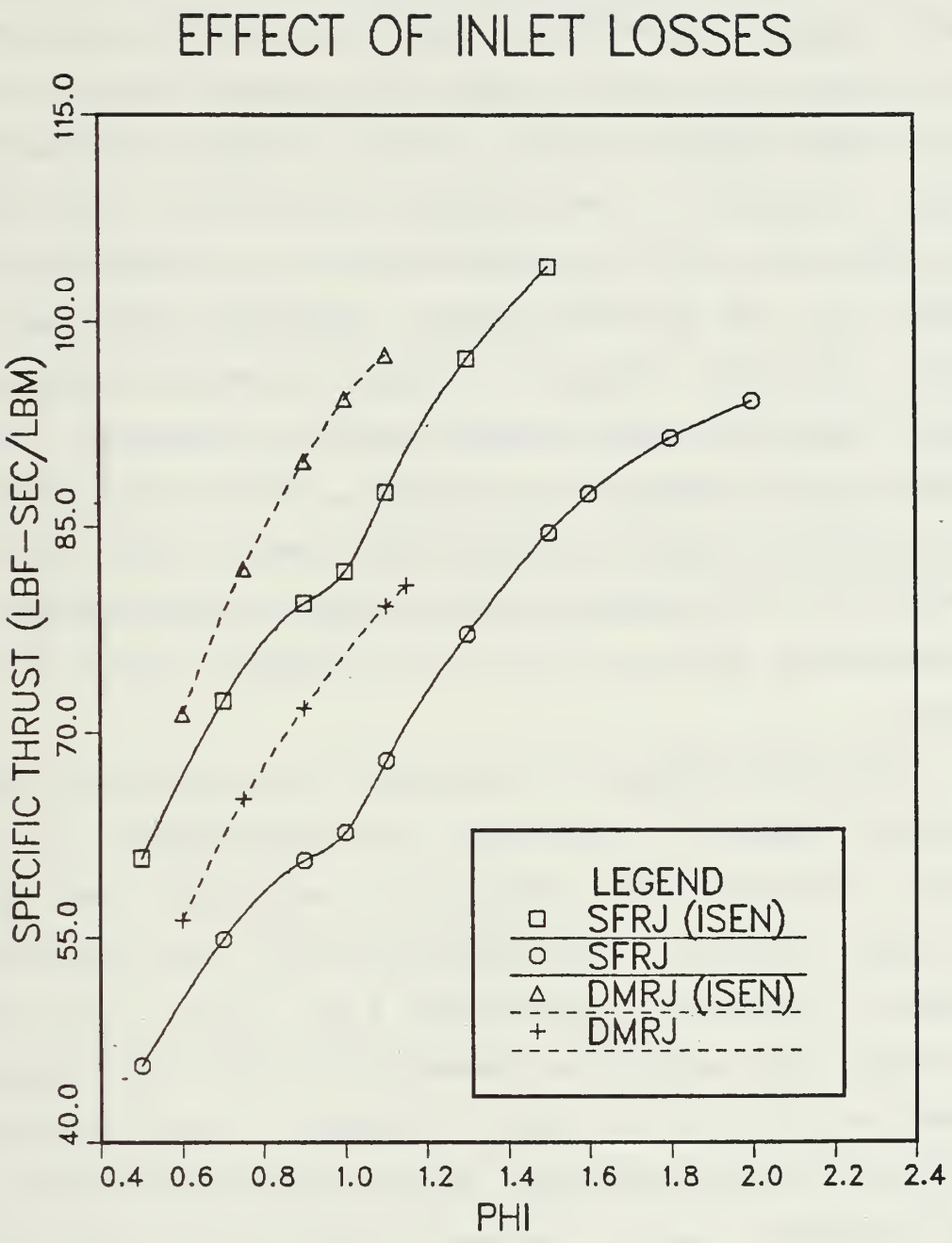

Figure 15 - Effect of using an isentropic inlet as compared to a wedge-type inlet.
(M_0 = 6.0, 80,000 ft., $\eta_{\Delta T}$ = 0.9 for DMRJ)

prevents complete combustion of the reactants by tying up chemical energy in intermediate species. Rather than a complete combustion process, where all of the fuel and oxidizer react to form CO_2 and H_2O, species such as OH, CO and H are present as well. Their presence reduces the potential temperature rise obtained by burning a specified amount of fuel and if recombination of the species is prevented in the exhaust nozzle, reducing the exhaust velocity. This can occur when kinetic rates and residence times are such that equilibrium cannot be attained. The limiting case is termed "frozen flow". When kinetic rates are fast enough compared to residence time in the combustor, "shifting equilibrium" exists, where recombination of the dissociated species allows more thermal energy to be released.

In using PEPCODE to determine the properties after equilibium adiabatic combustion, two approaches can be adopted. In this study, stagnation temperature was used as an input variable. This means that the gas properties are based on stagnation conditions, i.e., $M_4 = 0$. For the SFRJ, static and stagnation temperatures are very nearly the same so that it is not a problem. For the DMRJ, however, this is not the case. M_4 is supersonic, so that a large difference exists between static and stagnation properties. A more accurate method would be to use static temperature as the input variable in such a way that PEPCODE computes properties, based on shifting equilibrium, for $M_4 \neq 0$. This approach, while more accurate,

requires significantly more computation. For each data point, PEPCODE must be run twice, as well as RAMJET, to solve for the properties at the exit of the combustor.

This effect was examined and the results are presented in Figure 16 for an 80/20 DMRJ, with inlet losses, Mach 6, 80,000 ft. and $\eta_{\Delta T} = 0.9$. For $\Phi \leq 1$, using properties based on static conditions has no significant effect on the performance of the DMRJ. For $\Phi \geq 1.25$, i.e., fuel rich, properties based on static conditions would result in approximately 5% greater specific thrust. Since the anticipated range of equivalence ratios is from 0.8 to about 1.1, this effect was neglected and the properties were computed using stagnation conditions.

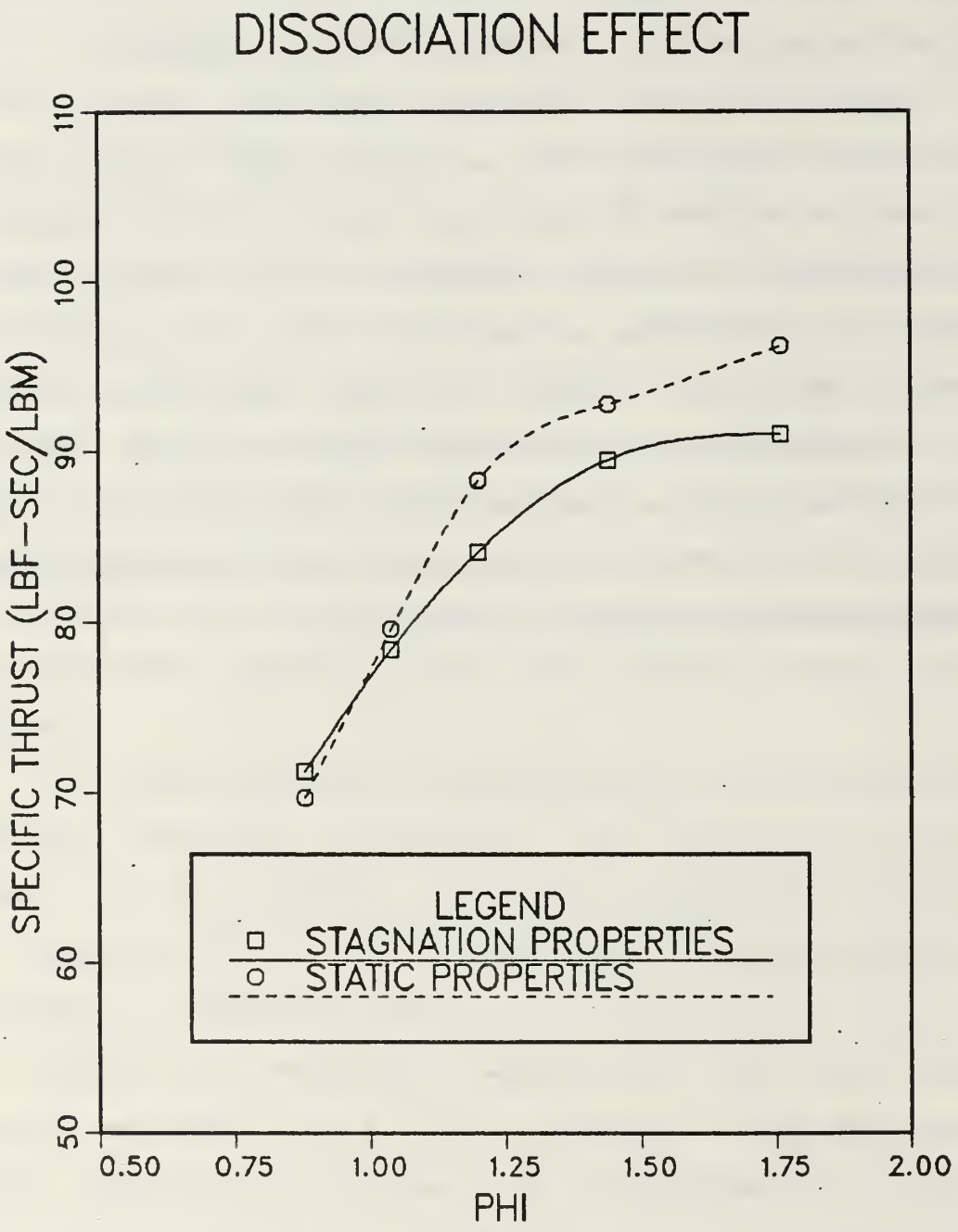

Figure 16 - Performance comparison between using properties computed by PEPCODE based on static conditions to properties based on stagnation conditions. (M_0 = 6.0, 80,000 ft., wedge-type inlet)

IV. EXPERIMENTAL PROCEDURE

The second objective of this study was to assess the feasibility of sustaining combustion in a supersonic flow, using a conventional SFRJ as a gas generator for a supersonic combustion chamber. A schematic of the apparatus is depicted in Figure 17. The apparatus was designed and constructed, however time constraints prohibited the tests from being conducted.

Two supplies of vitiated air were available, each producing a mass flow rate of 0.5 lbm/sec. The design parameters are listed below:

(a) $T = 1250^{\circ}R$ for both the primary air and bypass air.
(b) $P = 100$ psi for both streams entering the mixer.
(c) Mach number of 2.5 for both streams coming into the supersonic combustion chamber.
(d) $\Phi = 1.2$ in the SFRJ ($L_g = 10.59$ in.)
(e) Fuel : HTPB.

Because the kinetics of the mixing process was largely unknown, the streams were joined at an angle of 30° to force the mixing. The static pressures of the two streams entering the mixer were designed to be nearly equal in an effort to minimize losses. Shock losses were expected due to the large angle between flows, however these were

accepted in order to enhance the chances of mixing and combustion. The primary objective, initially, was just to obtain combustion, not necessarily efficient combustion.

The mixer length was determined from residence time considerations. Using an average Mach of 2.0, a mixer length of 6 feet should give a residence time of approximately 1.3 msec. Temperature and pressure readings would be made just entering the mixer and at the exit in order to ascertain whether or not sustained combustion occurred. If the engine successfully ignited and sustained combustion, the mixer would be shortened until combustion could not be attained. This would represent a measure of the kinetic rates of the reaction.

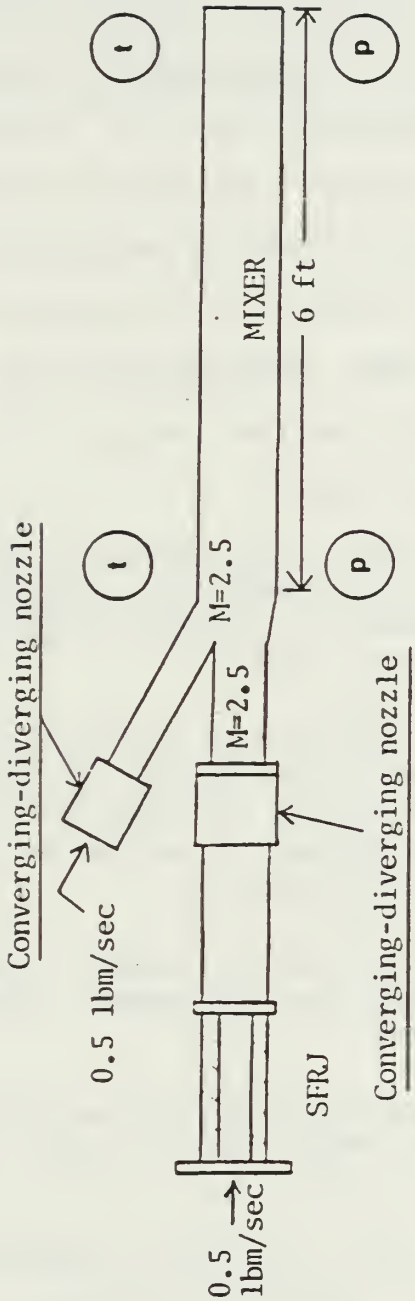

Figure 17 - Dual-mode combustor apparatus

V. CONCLUSIONS AND RECOMMENDATIONS

From an analytical standpoint, this study showed that a solid fuel, dual combustion mode ramjet exhibits areas of potential superior performance over a conventional solid fuel ramjet for use in a Mach 6 tactical missile. Based on the specified flight conditions and performance parameters, not accounting for any losses due to mixing in the supersonic combustor, the DMRJ outperforms the SFRJ at near stoichiometric equivalence ratios for $\eta_{\Delta T} > 0.5$. Additional results are summarized below:

(1) It is estimated that <u>with</u> mixing losses, combustion efficiency in the supersonic combustor must be at least 70% or greater to achieve superior performance with the DMRJ.

(2) For supersonic combustion efficiencies less than approximately 60%, performance of the DMRJ is very sensitive to the amount of airflow in the bypass stream. Greater bypass flow led to higher performance for the same overall Φ.

(3) The effect of decreasing inlet losses and lower Mach numbers were as expected; both leading to better performance.

(4) Dissociation effects proved to be relatively minor ($\approx$ 1%) in the range of Φ near stoichiometric (i.e., $\Phi \approx 0.8 - 1.1$).

In order to refine the range of required combustion efficiencies, follow-on research should focus on the actual mixing processes, the combustion kinetics and supersonic combustion processes. Experimental testing with

the completed DMRJ apparatus will provide insight into some of these areas, as well as some validation of the analytical model. Further studies should be conducted using solid fuels with different combustion efficiency characteristics than HTPB in order to more closely examine fuel effects on the system performance.

LIST OF REFERENCES

1. Jones, Robert A. and Huber, Paul W., Toward Scramjet Aircraft, Astronautics & Aeronautics, February 1978.

2. Billig, Frederick S., Tactical Missile Design Concepts, Vol. 4, Johns Hopkins APL Technical Digest, November 3, 1983.

3. Avery, W. H., Twenty-Five years of Ramjet Development, Vol. 25, No. 11, Jet Propulsion, November 1955.

4. Netzer, D. W., Overview of Tactical Missile Propulsion Design, Naval Postgraduate School, Monterey, CA.

5. Weber, Richard J. and MacKay, John S., "An Analysis of Ramjet Engines Using Supersonic Combustion", in Vol. 6, AIAA Selected Reprints, Ramjets, Gordon L. Dugger, ed., American Institute of Aeronautics and Astronautics June, 1969, pp. 102 - 110.

APPENDIX A - PEPCODE Data

TABLE 1

PEPCODE DATA FOR EQUILIBRIUM ADIABATIC COMBUSTION OF HTPB

Φ	f	γ	R	C_p	T_{4th}	γ_e	$C_{p\,e}$
0.5	.0367	1.266	53.256	.326	4746	1.297	.299
0.6	.0440	1.263	53.426	.330	4938	1.292	.304
0.7	.0514	1.260	53.689	.334	5088	1.289	.308
0.8	.0587	1.259	54.013	.338	5203	1.287	.311
0.85	.0624	1.258	54.199	.339	5251	1.286	.313
.9	.0661	1.258	54.415	.341	5292	1.286	.315
.95	.0697	1.258	54.631	.343	5325	1.285	.317
1.0	.0734	1.258	54.848	.344	5353	1.285	.318
1.05	.0771	1.258	55.095	.346	5375	1.285	.319
1.1	.0807	1.258	55.342	.347	5391	1.285	.321
1.15	.0844	1.258	55.605	.348	5402	1.286	.322
1.2	.0881	1.258	55.883	.350	5406	1.286	.323
1.25	.0918	1.259	56.176	.351	5405	1.287	.324
1.3	.0954	1.259	56.470	.352	5398	1.288	.325
1.4	.1028	1.261	57.119	.355	5365	1.290	.327
1.5	.1101	1.263	57.814	.357	5308	1.293	.328
1.6	.1174	1.265	58.540	.359	5230	1.296	.329
1.7	.1248	1.268	59.313	.361	5136	1.300	.330
1.8	.1321	1.271	60.101	.363	5031	1.304	.332
1.9	.1395	1.274	60.873	.364	4923	1.308	.332
2.0	.1468	1.277	61.676	.366	4809	1.312	.333
2.1	.1541	1.280	62.480	.367	4694	1.316	.334
2.2	.1615	1.283	63.268	.369	4581	1.32	.335
2.3	.1688	1.286	64.056	.370	4467	1.324	.336

Remarks:

1) All quantities in standard British units
2) P_2 = 120 psi; T = 3200°R
3) M_0 = 6.0; h = 80,000 ft
4) Exhaust data for frozen flow expansion

TABLE 2

PEPCODE DATA FOR EQUILIBRIUM ADIABATIC COMBUSTION OF HTPB

Φ	f	γ	R	C_p	T_{4th}	γ_e	C_{pe}
0.5	.0367	1.265	53.102	.326	4812	1.282	.311
0.6	.0440	1.261	53.194	.331	5041	1.276	.316
0.7	.0514	1.257	53.364	.335	5229	1.272	.321
0.8	.0587	1.255	53.612	.339	5378	1.269	.325
0.85	.0624	1.255	53.766	.341	5437	1.268	.327
0.9	.0661	1.254	53.951	.342	5489	1.268	.328
0.95	.0697	1.254	54.137	.344	5531	1.267	.330
1.0	.0734	1.254	54.353	.345	5565	1.267	.332
1.1	.0807	1.254	54.848	.348	5606	1.267	.334
1.2	.0881	1.255	55.404	.351	5614	1.268	.337
1.3	.0954	1.256	56.037	.353	5586	1.270	.339
1.35	.0991	1.257	56.393	.355	5559	1.271	.340
1.4	.1028	1.258	56.748	.356	5525	1.273	.340
1.45	.1064	1.259	57.119	.357	5484	1.274	.341
1.5	.1101	1.261	57.505	.358	5437	1.276	.342
1.6	.1174	1.263	58.293	.359	5332	1.280	.343
1.7	.1248	1.266	59.096	.361	5216	1.284	.344
1.8	.1321	1.269	59.931	.363	5094	1.288	.345
1.9	.1395	1.273	60.749	.365	4971	1.292	.346
2.0	.1468	1.276	61.568	.366	4848	1.296	.347
2.1	.1541	1.279	62.403	.368	4725	1.300	.348
2.2	.1615	1.282	63.191	.369	4606	1.304	.349
2.3	.1688	1.286	63.994	.370	4487	1.308	.349

Remarks:

1) All quantities in standard British units
2) P_2 = 620 psi; T = 3200°R
3) M_0 = 6.0; h = 80,000 ft; isentropic inlet
4) Exhaust data for frozen flow expansion

TABLE 3

PEPCODE DATA FOR EQUILIBRIUM ADIABATIC COMBUSTION OF HTPB

Φ	f	γ	R	C_p	T_{4th}	γ_e	C_{pe}
0.6	.0440	1.267	52.876	.323	3946	1.295	.298
0.7	.0514	1.261	52.913	.329	4218	1.288	.304
0.8	.0587	1.257	53.035	.334	4436	1.282	.310
0.9	.0661	1.254	53.295	.338	4595	1.279	.314
1.0	.0734	1.253	53.673	.341	4694	1.277	.318
1.1	.0807	1.254	54.183	.344	4735	1.278	.320
1.2	.0881	1.255	54.826	.347	4718	1.280	.322
1.3	.0954	1.258	55.570	.348	4648	1.284	.323
1.4	.1028	1.261	56.389	.350	4546	1.289	.324
1.5	.1101	1.266	57.357	.351	4415	1.294	.324
1.6	.1174	1.269	58.098	.352	4302	1.299	.324
1.7	.1248	1.273	58.956	.353	4178	1.304	.325
1.8	.1321	1.277	59.806	.354	4052	1.309	.325
1.9	.1395	1.281	60.640	.355	3932	1.314	.326
2.0	.1468	1.285	61.498	.356	3810	1.319	.327
2.1	.1541	1.289	62.333	.357	3690	1.324	.327
2.2	.1615	1.294	63.144	.358	3576	1.329	.328

Remarks:

1) All quantities in standard British units
2) P_2 = 50 psi; T = 1640°R
3) M_0 = 4.0; h = 80,000 ft
4) Exhaust data for frozen flow expansion

APPENDIX B - RAMJET

```
      PROGRAM RAMJET
**********************************************************************
**  PROGRAM USED TO DETERMINE THE EXIT CONDITIONS OF A RAMJET BURNER **
**  CHAMBER.  A LEGEND FOR THE VARIABLES INVOLVED IS OFFERED BELOW.  **
**                                                                  **
**  STATION 0: FREESTREAM CONDITIONS                                **
**  STATION 2: INPUT CONDITIONS FOR THE COMBUSTION CHAMBER          **
**  STATION 4: EXIT CONDITIONS OF COMBUSTION CHAMBER                **
**  STATION E: EXHAUST CONDITIONS(POST NOZZLE)                      **
**                                                                  **
**  M: MACH NUMBER                                                  **
**  T: STATIC TEMPERATURE (DEG R)                                   **
**  TT:TOTAL TEMP (DEG R)                                           **
**  P: STATIC PRESSURE (LBF/IN2)                                    **
**  PT:TOTAL PRESSURE (LBF/IN2)                                     **
**  GAMMA: RATIO OF SPECIFIC HEATS                                  **
**  R: GAS CONSTANT (BTU/LBM-DEG R)                                 **
**  CP:SPECIFIC HEAT (BTU/LBM-DEG R)                                **
**  F: FUEL TO AIR RATIO                                            **
**  PHI: EQUIVALENCE RATIO                                          **
**  MDOT: MASS FLOW RATE (LBM/SEC)                                  **
**  U: FLUID VELOCITY (FT/SEC)                                      **
**  GC: PROPORTIONALITY CONSTANT (FT-LBF/LBM-SEC2)                  **
**  J: CONVERSION FACTOR = 778 BTU/FT-LBF                           **
**  DELTA: CONVERGENCE LIMIT                                        **
**  D: PORT DIAMETER (IN)                                           **
**  STEP: MACH NO. INCREMENT                                        **
**  THRUST: UNINSTALLED THRUST (LBF)                                **
**  STHRST: SPECIFIC THRUST (LBF-SEC/LBM)                           **
**  SFC: SPECIFIC FUEL CONSUMPTION (LBM/LBF-SEC)                    **
**  ETA: THERMAL EFFICIENCY (TEMPERATURE RISE)                      **
**                                                                  **
**********************************************************************
```

```
C
C
      DOUBLE   PRECISION   P0,P2,P4,PT0,PT2,PT4,T0,T2,T4,TT0,TT2,TT4,M2,M4
      DOUBLE  PRECISION  CP2,CP4,GAMMA2,GAMMA4,R2,R4,F,H,MDOT0,GC,CD,U2
      DOUBLE  PRECISION  U4,TEST,DELTA,MDOT4,STEP,DELTT,M0,UE,U0,THRUST
      DOUBLE  PRECISION  STHRST,D2,D4,PI,GAMMAE,ME,TE,PE,PTE,TTE,ETA
      DOUBLE PRECISION TT4TH,J,CPE,PHI,SFC
      CHARACTER*1 ANS, ANSWER
100    PRINT *,'ALL UNITS ARE STANDARD ENGLISH UNITS'
C-----INITIAL DATA
      DATA M0,P0,T0/6,.404,390/
      DATA CD,GC,DELTA,STEP/1.5,32.174,.0001,.00001/
      DATA M2,GAMMA0,R0,CP0,D2/.2000,1.40,53.3,.24,1.674/
      DATA R2,CP2,GAMMA2/53.3,.28,1.33/
      DATA J,PT2,MDOT0/778,146.72,1.00D0/
      PE = P0
      PI=ASIN(1.D0)*2.D0
      A2= (PI/4.D0)*D2*D2
      PRINT *,'A2=',A2
C-----CONSTANT AREA COMBUSTOR
      A4=A2
C-----INITIAL FLOW COMPUTATIONS
      PT0=P0*(1.+M0*M0*(GAMMA0-1.)*.5)**(GAMMA0/(GAMMA0-1.))
      TT0=T0*(1.+M0*M0*(GAMMA0-1.)*.5)
      TT2=TT0
      T2=TT2/(1.+M2*M2*(GAMMA2-1.)*.5)
      P2=PT2/((1.+M2*M2*(GAMMA2-1.)*.5)**(GAMMA2/(GAMMA2-1.)))
      PRINT 5,'P2=',P2
5      FORMAT(1X,A3,F9.4)
      PRINT 6,'T2=',T2
6      FORMAT(1X,A3,F9.4)
C-----INITIAL GUESS ON EXIT MACH
50     PRINT *, 'INPUT ESTIMATE OF M4'
      READ *, M4
C-----INPUT PEPCODE DATA
```

```
      PRINT *,'INPUT TT4TH(DEG R)'
      READ *, TT4TH
      PRINT *,'INPUT GAS PROPERTIES (F,R4,CP4,GAMMA4,GAMMAE)'
      READ *, F,R4,CP4,GAMMA4,GAMMAE
      PHI = F/0.0734D0
C-----DETERMINE ETA FOR HTPB
      IF (PHI .LE. 1) THEN
         ETA = 1.D0 - .35D0*PHI**.92D0
      ELSE
         ETA = .3D0 + .35D0*PHI**.92D0
      END IF
C-----SOLVE FOR M4
      TT4 = ETA*(TT4TH - TT2) + TT2
10     IF (M4 .GE. .999) THEN
         PRINT *,'FLOW IS CHOKED FOR THIS VALUE OF F'
         GOTO 50
      ENDIF
      CPE = R4*GAMMAE/((GAMMAE-1.D0)*J)
      T4=TT4/(1.+M4*M4*(GAMMA4-1.)*.5)
      U4=M4*SQRT(GC*GAMMA4*R4*T4)
      U2=M2*SQRT(GC*GAMMA2*R2*T2)
C-----MOMENTUM EQUATION FOR P4
      P4=P2+(MDOT0*(U2-(1.+F)*U4))/(GC*A2)-CD*P2*U2*U2/(2.*R2*T2*GC)
      PT4=P4*(1.+M4*M4*(GAMMA4-1.)*.5)**(GAMMA4/(GAMMA4-1.))
      MDOT4=MDOT0*(1.+F)
      TEST = MDOT4 - P4*A4*U4/(R4*T4)
C-----CHECK GUESS ON M4
      IF (ABS(TEST) .GE. DELTA) THEN
         M4=M4+STEP
         GOTO 10
      END IF
C-----SOLVE FOR EXIT CONDITIONS
      ME=SQRT((2.D0/(GAMMAE  -  1.D0)*((PT4/PE)**((GAMMAE-1.D0)/GAMMAE)
     + - 1.D0)))
      UE=SQRT(2.*GC*J*CPE*TT4*(1.-(PE/PT4)**((GAMMAE-1.)/GAMMAE)))
```

```
      TE=TT4/(1.D0+ME*ME*(GAMMAE-1.D0)*.5D0)
      U0=M0*SQRT(GC*GAMMA0*R2*T0)
      THRUST=(MDOT4*UE-MDOT0*U0)/GC
      STHRST=THRUST/MDOT0
      SFC = F/STHRST
      PRINT 15,'M0','M2','M4','ME'
15    FORMAT(/1X,4A9)
      PRINT 20,M0,M2,M4,ME
20    FORMAT(1X,4F9.3/)
      PRINT 25,'T0','T2','T4','TE'
25    FORMAT(1X,4A9)
      PRINT 30,T0,T2,T4,TE
30    FORMAT(1X,4F9.1/)
      PRINT 35,'TT0','TT2','TT4','TTE'
35    FORMAT(1X,4A9)
      PRINT 40,TT0,TT2,TT4,TT4
40    FORMAT(1X,4F9.1/)
      PRINT 45,'P0','P2','P4','PE'
45    FORMAT(1X,4A9)
      PRINT 60,P0,P2,P4,PE
60    FORMAT(1X,4F9.3/)
      PRINT 65,'PT0','PT2','PT4','PTE'
65    FORMAT(1X,4A9)
      PRINT 70,PT0,PT2,PT4,PT4
70    FORMAT(1X,4F9.3/)
      PRINT 75,'U0','U2','U4','UE'
75    FORMAT(1X,4A9)
      PRINT 80,U0,U2,U4,UE
80    FORMAT(1X,4F9.3/)
      PRINT 85,'F','MDOT0','THRUST','SPTHRUST','SFC'
85    FORMAT(1X,5A9)
      PRINT 90,F,MDOT0,THRUST,STHRST,SFC
90    FORMAT(1X,4F9.4,F10.6/)
      WRITE (*,*) 'PERFORM ANOTHER RUN THIS FLIGHT CONDITION (Y/N)?'
      READ (*,'(A)') ANS
```

```
      IF (ANS .EQ. 'N') GOTO 110
      GOTO 50
110   WRITE (*,*) 'START NEW PROBLEM (Y/N)?'
      READ (*,'(A)') ANSWER
      IF (ANSWER .EQ. 'N') STOP
      GOTO 100
      END
```

SAMPLE OUTPUT:

```
run raml fortran
VS FORTRAN COMPILER ENTERED.  14:06:42

**RAMJET** END OF COMPILATION 1 ******
VS FORTRAN COMPILER EXITED.   14:06:45


EXECUTION BEGINS...
ALL UNITS ARE STANDARD ENGLISH UNITS
A2=  2.20090103
P2= 142.8812
T2=3177.0289
INPUT ESTIMATE OF M4
?
.25
INPUT TT4TH(DEG R)
?
5353
INPUT GAS PROPERTIES (F,R4,CP4,GAMMA4,GAMMAE)
?
.0734,54.848,.344,1.258,1.285

       M0        M2        M4        ME
    6.000     0.200     0.293     4.309

       T0        T2        T4        TE
    390.0    3177.0    4548.4    1261.3

      TT0       TT2       TT4       TTE
   3198.0    3198.0    4598.7    4598.7

       P0        P2        P4        PE
    0.404   142.881   130.670     0.404

      PT0       PT2       PT4       PTE
  637.867   146.720   137.879   137.879

       U0        U2        U4        UE
 5805.821   538.372   931.042  7287.592

        F     MDOT0    THRUST SPTHRUST       SFC
   0.0734    1.0000   62.6804   62.6804  0.001171

PERFORM ANOTHER RUN THIS FLIGHT CONDITION (Y/N)?
n
START NEW PROBLEM (Y/N)?
n
R; T=0.97/1.54 14:07:18
```

APPENDIX C - MIXER

```
      PROGRAM MIXER
C
      CHARACTER ANS
      REAL ETA,M4,T4TH,TT4TH,TT4,T4,PT4,P4,A4,A3A,A3B,GAMMA4,R4,CP4
      REAL TT3A,TT3B,TT3BAR,U3A,U3B,U4,MDOT3A,MDOT3B,MDOT4,GC
      REAL FNT,FNIT,FNU,FNA,FNGAM,FNP,P3A,P3B,V4,DELPA,DIFF
C-----INPUT ALL THE PERTINENT DATA
      PRINT *,'INPUT R4,GAMMA4,T4TH'
      READ *,R4,GAMMA4,T4TH
      PRINT *, 'INPUT MDOT3A,MDOT3B,TT3A,TT3B'
      READ *, MDOT3A,MDOT3B,TT3A,TT3B
      PRINT *,'INPUT P3A,P3B,A3A,A3B'
      READ *,P3A,P3B,A3A,A3B
      PRINT *,'INPUT U3A,U3B'
      READ *,U3A,U3B
10     PRINT *, 'INPUT ETA,M4'
      READ *, ETA,M4
C
      GC = 32.174
      TT4TH = FNIT(T4TH,GAMMA4,M4)
      MDOT4 = MDOT3A+MDOT3B
      TT3BAR =(MDOT3A*TT3A + MDOT3B*TT3B)/MDOT4
      TT4 = (TT4TH - TT3BAR)*ETA + TT3BAR
      T4 = FNT(TT4,GAMMA4,M4)
      U4 = FNU(GAMMA4,R4,T4,M4)
C
      A4 = A3A + A3B
      PT4 = (MDOT4*SQRT(TT4)*FNA(GAMMA4,M4))/(A4*FNGAM(GAMMA4,R4))
      P4 = FNP(M4,PT4,GAMMA4)
      DELPA = P3A*A3A + P3B*A3B - P4*A4
      V4 = (.9*GC*DELPA + MDOT3A*U3A + MDOT3B*U3B)/MDOT4
      DIFF = (U4 - V4)
      PRINT 15,TT3BAR
```

```
15    FORMAT(1X,'TT3BAR =',F9.3)
      PRINT 20,TT4TH
20    FORMAT(1X,'TT4TH  =',F9.3)
      PRINT 25,TT4
25    FORMAT(1X,'TT4    =',F9.3)
      PRINT 30,T4
30    FORMAT(1X,'T4     =',F9.3)
      PRINT 35,U4
35    FORMAT(1X,'U4     =',F9.3)
      PRINT 40,PT4
40    FORMAT(1X,'PT4    =',F9.3)
      PRINT 45,P4
45    FORMAT(1X,'P4     =',F9.3)
      PRINT 50,V4
50    FORMAT(1X,'V4     =',F9.3)
      PRINT 55,DIFF
55    FORMAT(1X,'U4-V4  =',F9.3)
      IF (ABS(DIFF) .LT. .01) STOP
      PRINT *,'CONTINUE? (Y/N)'
      READ (*,'(A)')  ANS
      IF (ANS .EQ. 'N') STOP
      GOTO 10
      END
*******FNTT*************************************************************
***    THIS FUNCTION DETERMINES STAGNATION TEMPERATURE (DEG R) GIVEN ***
***    STATIC TEMPERATURE, MACH AND GAMMA.                           ***
************************************************************************
      FUNCTION FNTT(T,GAM,M)
      REAL T,GAM,M
      FNTT= T*(1.+.5*M*M*(GAM - 1.))
      END
******FNT***************************************************************
***    THIS FUNCTION DETERMINES STATIC TEMPERATURE GIVEN MACH, GAMMA ***
***    AND STAGNATION TEMPERATURE.                                   ***
```

```
************************************************************************
      FUNCTION FNT(TT,GAM,M)
      REAL TT,GAM,M
      FNT =  TT/(1.+.5*M*M*(GAM - 1.))
      END
******FNU*************************************************************
***   THIS FUNCTION DETERMINES GAS VELOCITY GIVEN GAMMA, GAS CONSTANT ***
***   STATIC TEMPERATURE AND MACH.                                    ***
************************************************************************
      FUNCTION FNU(GAM,R,T,M)
      REAL GAM,R,T,M,GC
      GC = 32.174
      FNU = M*SQRT(GC*R*GAM*T)
      END
******FNA*************************************************************
***    THIS FUNCTION DETERMINES THE RATIO A/A* GIVEN MACH AND GAMMA. ***
************************************************************************
      FUNCTION FNA(GAM,M)
      REAL GAM,M
      FNA  =  (1.0/M)*((2.0/(GAM+1.0))*(1.0+.5*M*M*(GAM  -  1.0)))**((GAM
     +       +1.0)/(2.0*(GAM - 1.0)))
      END
*****FNGAM************************************************************
*** THIS FUNCTION IS THE FUNCTION OF GAMMA AND R IN THE CONTINUITY  ***
*** EQUATION.                                                       ***
************************************************************************
      FUNCTION FNGAM(GAM,R)
      REAL GAM,R,GC
      GC = 32.174
      FNGAM =  SQRT((GAM*GC/R)*(2.0/(GAM+1.0))**((GAM + 1.)/(GAM - 1.)))
      END
******FNP*************************************************************
***    THIS FUNCTION DETERMINES THE STATIC PRESSURE GIVEN GAMMA, MACH **
***    AND STAGNATION PRESSURE.                                        **
************************************************************************
```

```
      FUNCTION FNP(M,PT,GAM)
      REAL M,GAM,PT
      FNP = PT/(1.0 + .5*M*M*(GAM - 1.0))**(GAM/(GAM - 1.))
      END
```

SAMPLE OUTPUT:

```
run mixer fortran
VS FORTRAN COMPILER ENTERED.  14:12:36
**MIXER** END OF COMPILATION 1 ******
**FNTT** END OF COMPILATION 2 ******
**FNT** END OF COMPILATION 3 ******
**FNU** END OF COMPILATION 4 ******
**FNA** END OF COMPILATION 5 ******
**FNGAM** END OF COMPILATION 6 ******
**FNP** END OF COMPILATION 7 ******
**FNPT** END OF COMPILATION 8 ******
VS FORTRAN COMPILER EXITED.   14:12:54

EXECUTION BEGINS...
INPUT R4,GAMMA4,TT4TH
?
54.415,1.258,5292
INPUT CP3A,CP3B,CP4
?
.248,.332,.341
INPUT MDOT3A,MDOT3B,TT3A,TT3B
?
.5,.5661,3198,4849.5
INPUT P3A,P3B,A3A,A3B
?
16.4,16.4,.517,1.103
INPUT U3A,U3B
?
4666.61,5594.2
INPUT M4
?
1.423

TT3BAR = 4193.020
TT4TH  = 5292.000
TT4    = 5182.102
T4     = 4108.812
U4     = 4280.703
PT4    =  106.573
P4     =   34.372
V4     = 4280.520
U4-V4  =    0.184
MDOT4* =   1.0660
MDOT4  =   1.0661
CONTINUE? (Y/N)
n
R; T=0.58/1.46 14:13:56
```

APPENDIX D - SFRJ Properties

TABLE 4

PROPERTIES THROUGH SFRJ

Φ	.50	.70	1.00	1.30	1.80
$\eta_{\Delta T}$	.82	.75	.65	.75	.90
m_0	1.00	1.00	1.00	1.00	1.00
m_f	.04	.05	.07	.10	.13
T_2	3198.00	3198.00	3198.00	3198.00	3198.00
T_4	4459.70	4611.40	4598.70	4838.00	4849.50
M_4	.27	.28	.29	.32	.34
t_4	4416.80	4564.10	4548.40	4776.40	4773.90
P_0	637.87	637.87	637.87	637.87	637.87
P_2	146.73	146.73	146.73	146.73	146.73
P_4	138.79	138.32	137.89	136.93	135.70
p_0	.40	.40	.40	.40	.40
p_2	142.89	142.89	142.89	142.89	142.89
p_4	132.56	131.58	130.68	128.65	126.07
u_0	5805.80	5805.80	5805.80	5805.80	5805.80
u_2	538.37	538.37	538.37	538.37	538.37
u_4	835.77	889.56	930.98	1043.38	1170.58
u_e	7015.31	7201.00	7287.61	7566.49	7727.80
F	45.59	54.86	62.68	77.16	91.47
S	8.0492e-4	9.3650e-4	1.1710e-3	1.2366e-3	1.4444e-3

Remarks:

1) $M_0 = 6.0$; h = 80,000 ft
2) $\eta_{\Delta T} = fn(\Phi)$
3) All quantites in standard British units

TABLE 5

PROPERTIES THROUGH SFRJ

Φ	.50	.70	1.00	1.30	1.50
$\eta_{\Delta T}$	.82	.75	.65	.75	.81
m_0	1.00	1.00	1.00	1.00	1.00
m_f	.04	.05	.07	.10	.11
T_2	3198.00	3198.00	3198.00	3198.00	3198.00
T_4	4513.40	4716.80	4736.50	4978.20	5007.70
M_4	.27	.29	.30	.32	.33
t_4	4469.80	4668.00	4684.10	4913.70	4936.80
P_0	637.87	637.87	637.87	637.87	637.87
P_2	637.87	637.87	637.87	637.87	637.87
P_4	603.09	600.82	598.77	594.47	592.16
p_0	.40	.40	.40	.40	.40
p_2	621.18	621.18	621.18	621.18	621.18
p_4	575.75	571.00	566.72	557.64	552.74
u_0	5805.80	5805.80	5805.80	5805.80	5805.80
u_2	538.37	538.37	538.37	538.37	538.37
u_4	843.85	905.64	952.10	1067.93	1125.72
u_e	7487.60	7736.89	7857.18	8156.33	8244.19
F	60.81	72.38	81.68	97.25	104.00
S	6.0349e-4	7.0991e-4	8.9859e-4	9.8122e-4	1.0587e-3

Remarks:

1) $M_0 = 6.0$; h = 80,000 ft
2) $\eta_{\Delta T}$ = fn(Φ)
3) All quantites in standard British units
4) Isentropic inlet

TABLE 6

PROPERTIES THROUGH SFRJ

Φ	.70	.90	1.10	1.30	1.80
$\eta_{\Delta T}$	.75	.68	.68	.75	.90
m_0	1.00	1.00	1.00	1.00	1.00
m_f	.05	.07	.08	.10	.13
T_2	1638.00	1638.00	1638.00	1638.00	1638.00
T_4	3567.40	3655.10	3749.80	3881.80	3813.00
M_4	.37	.39	.41	.44	.48
t_4	3504.30	3586.50	3672.10	3789.20	3696.50
P_0	61.34	61.34	61.34	61.34	61.34
P_2	31.95	31.95	31.95	31.95	31.95
P_4	29.26	29.11	28.91	28.63	28.18
p_0	.404	.404	.404	.404	.404
p_2	31.09	31.09	31.09	31.09	31.09
p_4	26.85	26.51	26.07	25.45	24.42
u_0	3870.55	3870.55	3870.55	3870.55	3870.55
u_2	390.90	390.90	390.90	390.90	390.90
u_4	1018.35	1078.20	1156.89	1271.23	1437.11
u_e	5785.54	5904.23	6030.25	6188.78	6272.16
F	68.76	75.33	82.26	90.41	100.40
S	7.4725e-4	8.7692e-4	9.8154e-4	1.0554e-3	1.3159e-3

Remarks:

1) $M_0 = 4.0$; h = 80,000 ft
2) $\eta_{\Delta T} = fn(\Phi)$
3) All quantites in standard British units

APPENDIX E - DMRJ Properties

TABLE 7

PROPERTIES THROUGH DMRJ (50/50)

Φ_{SFRJ}	1.20	1.50	1.80	2.20	2.30
Φ_{TOT}	.60	.75	.90	1.10	1.15
m_{3A}	.50	.50	.50	.50	.50
m_{3B}	.54	.56	.57	.58	.58
T_{3A}	3198.00	3198.00	3198.00	3198.00	3198.00
T_{3B}	4774.50	4903.40	4849.50	4612.80	4534.30
T_4	4856.42	5056.25	5182.10	5258.11	5263.50
M_{3B}	2.06	2.05	2.05	2.04	2.04
M_4	1.54	1.49	1.42	1.30	1.27
t_{3B}	2976.70	3034.30	2922.50	2766.30	2706.50
t_4	3701.93	3927.17	4108.81	4312.30	4359.34
P_0	637.87	637.87	637.87	637.87	637.87
P_{2A}	281.96	281.96	281.96	281.96	281.96
P_{2B}	146.73	146.73	146.73	146.73	146.73
P_{3A}	281.96	281.96	281.96	281.96	281.96
P_{3B}	138.01	136.36	135.72	135.17	135.09
P_4	113.06	109.98	106.57	102.67	101.72
p_0	.40	.40	.40	.40	.40
p_{3A}	16.40	16.40	16.40	16.40	16.40
p_{3B}	16.40	16.40	16.40	16.40	16.40
p_4	30.70	32.20	34.37	39.04	40.58
u_{3A}	4666.61	4666.61	4666.61	4666.61	4666.61
u_{3B}	5391.56	5539.50	5594.20	5568.70	5548.60
u_4	4365.81	4630.70	4280.70	4052.73	3971.72
u_e	7295.48	7488.00	7620.32	7730.24	7748.30
u_0	5805.80	5805.80	5805.80	5805.80	5805.80
F	56.28	65.11	72.05	79.20	80.70
S	7.8183e-4	8.4626e-4	9.1738e-4	1.0194e-3	1.0458e-3

Remarks:

1) $M_0 = 6.0$; h = 80,000 ft

2) $\eta_{\Delta T} = 0.9$

TABLE 8

PROPERTIES THROUGH DMRJ (50/50)

Φ_{SFRJ}	1.20	1.50	1.80	2.20	2.30
Φ_{TOT}	.60	.75	.90	1.10	1.15
m_{3A}	.50	.50	.50	.50	.50
m_{3B}	.54	.56	.57	.58	.58
T_{3A}	3198.00	3198.00	3198.00	3198.00	3198.00
T_{3B}	4774.50	4903.40	4849.50	4612.80	4534.30
T_4	4611.70	4774.99	4852.41	4859.43	4848.02
M_{3B}	2.06	2.05	2.05	2.04	2.04
M_4	1.69	1.66	1.62	1.55	1.53
t_{3B}	2976.70	3034.30	2922.50	2766.30	2706.50
t_4	3352.56	3523.64	3628.52	3708.57	3721.33
P_0	637.87	637.87	637.87	637.87	637.87
P_{2A}	281.96	281.96	281.96	281.96	281.96
P_{2B}	146.73	146.73	146.73	146.73	146.73
P_{3A}	281.96	281.96	281.96	281.96	281.96
P_{3B}	138.01	136.36	135.72	135.17	135.09
P_4	123.12	120.22	117.27	113.69	112.69
p_0	.40	.40	.40	.40	.40
p_{3A}	16.40	16.40	16.40	16.40	16.40
p_{3B}	16.40	16.40	16.40	16.40	16.40
p_4	26.63	27.44	28.43	30.44	31.03
u_{3A}	4666.61	4666.61	4666.61	4666.61	4666.61
u_{3B}	5391.56	5539.50	5594.20	5568.70	5548.60
u_4	4559.37	4590.77	4571.16	4470.29	4433.61
u_e	7135.60	7305.35	7405.50	7465.70	7470.70
u_0	5805.80	5805.80	5805.80	5805.80	5805.80
F	51.09	59.12	64.93	70.33	71.34
S	8.6123e-4	9.3203e-4	1.0179e-3	1.1481e-3	1.1830e-3

Remarks:

1) $M_0 = 6.0$; h = 80,000 ft

2) $\eta_{\Delta T} = 0.6$

TABLE 9

PROPERTIES THROUGH DMRJ (50/50)

Φ_{SFRJ}	1.20	1.50	1.80	2.20	2.30
Φ_{TOT}	.60	.75	.90	1.10	1.15
m_{3A}	.50	.50	.50	.50	.50
m_{3B}	.54	.56	.57	.58	.58
T_{3A}	3198.00	3198.00	3198.00	3198.00	3198.00
T_{3B}	4774.50	4903.40	4849.50	4612.80	4534.30
T_4	4530.13	4681.24	4742.51	4726.53	4709.53
M_{3B}	2.06	2.05	2.05	2.04	2.04
M_4	1.74	1.71	1.68	1.63	1.62
t_{3B}	2976.70	3034.30	2922.50	2766.30	2706.50
t_4	3239.07	3392.20	3473.37	3518.96	3522.78
P_0	637.87	637.87	637.87	637.87	637.87
P_{2A}	281.96	281.96	281.96	281.96	281.96
P_{2B}	146.73	146.73	146.73	146.73	146.73
P_{3A}	281.96	281.96	281.96	281.96	281.96
P_{3B}	138.01	136.36	135.72	135.17	135.09
P_4	127.22	124.57	122.00	118.82	117.90
p_0	.40	.40	.40	.40	.40
p_{3A}	16.40	16.40	16.40	16.40	16.40
p_{3B}	16.40	16.40	16.40	16.40	16.40
p_4	25.40	26.03	26.72	28.19	28.62
u_{3A}	4666.61	4666.61	4666.61	4666.61	4666.61
u_{3B}	5391.56	5539.50	5594.20	5568.70	5548.60
u_4	4616.78	4659.38	4654.91	4579.11	4550.24
u_e	7082.10	7244.40	7333.80	7377.30	7378.00
u_0	5805.80	5805.80	5805.80	5805.80	5805.80
F	49.35	57.12	62.56	67.36	68.22
S	8.9152e-4	9.6464e-4	1.0566e-3	1.1987e-3	1.2372e-3

Remarks:

1) $M_0 = 6.0$; h = 80,000 ft
2) $\eta_{\Delta T} = 0.5$

TABLE 10

PROPERTIES THROUGH DMRJ (50/50)

Φ_{SFRJ}	1.20	1.50	1.80	2.20	2.30
Φ_{TOT}	.60	.75	.90	1.10	1.15
m_{3A}	.50	.50	.50	.50	.50
m_{3B}	.54	.56	.57	.58	.58
T_{3A}	3198.00	3198.00	3198.00	3198.00	3198.00
T_{3B}	4774.50	4903.40	4849.50	4612.80	4534.30
T_4	4326.19	4446.86	4467.76	4394.30	4363.30
M_{3B}	2.06	2.05	2.05	2.04	2.04
M_4	1.88	1.86	1.86	1.84	1.84
t_{3B}	2976.70	3034.30	2922.50	2766.30	2706.50
t_4	2957.48	3068.96	3094.25	3058.51	3040.95
P_0	637.87	637.87	637.87	637.87	637.87
P_{2A}	281.96	281.96	281.96	281.96	281.96
P_{2B}	146.73	146.73	146.73	146.73	146.73
P_{3A}	281.96	281.96	281.96	281.96	281.96
P_{3B}	138.01	136.36	135.72	135.17	135.09
P_4	139.95	138.17	137.20	136.36	136.12
p_0	.40	.40	.40	.40	.40
p_{3A}	16.40	16.40	16.40	16.40	16.40
p_{3B}	16.40	16.40	16.40	16.40	16.40
p_4	22.53	22.78	22.88	23.30	23.41
u_{3A}	4666.61	4666.61	4666.61	4666.61	4666.61
u_{3B}	5391.56	5539.50	5594.20	5568.70	5548.60
u_4	4753.61	4817.32	4842.54	4816.07	4803.16
u_e	6948.42	7091.72	7153.93	7155.51	7145.50
u_0	5805.80	5805.80	5805.80	5805.80	5805.80
F	45.02	52.11	56.60	59.91	60.38
S	9.7743e-4	1.0573e-3	1.1679e-3	1.3478e-3	1.3977e-3

Remarks:

1) $M_0 = 6.0$; h = 80,000 ft
2) $\eta_{\Delta T} = 0.25$

TABLE 11

PROPERTIES THROUGH DMRJ (80/20)

Φ_{SFRJ}	1.10	1.30	1.50	1.80	2.20
Φ_{TOT}	.88	1.04	1.20	1.44	1.76
m_{3A}	.20	.20	.20	.20	.20
m_{3B}	.86	.88	.89	.91	.93
T_{3A}	3198.00	3198.00	3198.00	3198.00	3198.00
T_{3B}	4693.40	4838.00	4903.40	4849.50	4612.80
T_4	5194.71	5293.01	5330.93	5271.16	5007.53
M_{3B}	2.057	2.05	2.05	2.05	2.04
M_4	1.56	1.58	1.60	1.61	1.62
t_{3B}	2928.40	3010.20	3034.30	2963.10	2753.00
t_4	3958.40	4001.22	4009.98	3936.22	3714.24
P_0	637.87	637.87	637.87	637.87	637.87
P_{2A}	281.96	281.96	281.96	281.96	281.96
P_{2B}	146.73	146.73	146.73	146.73	146.73
P_{3A}	281.96	281.96	281.96	281.96	281.96
P_{3B}	137.56	136.92	136.35	135.71	135.16
P_4	103.60	104.79	105.61	106.43	107.50
p_0	.40	.40	.40	.40	.40
p_{3A}	16.40	16.40	16.40	16.40	16.40
p_{3B}	16.40	16.40	16.40	16.40	16.40
p_4	27.53	26.78	26.35	26.07	26.04
u_{3A}	4666.61	4666.61	4666.61	4666.61	4666.61
u_{3B}	5323.47	5450.17	5539.40	5594.10	5562.50
u_4	4590.69	4723.43	4812.61	4873.04	4859.37
u_e	7607.70	7738.90	7823.28	7856.59	7736.12
u_0	5805.80	5805.80	5805.80	5805.80	5805.80
F	71.28	78.44	84.13	89.55	91.06
S	9.0629e-4	9.7278e-4	1.0472e-3	1.1803e-3	1.4188e-3

Remarks:

1) $M_0 = 6.0$; h = 80,000 ft
2) $\eta_{\Delta T} = 0.9$

TABLE 12

PROPERTIES THROUGH DMRJ (80/20)

Φ_{SFRJ}	1.10	1.30	1.50	1.80	2.20
Φ_{TOT}	.88	1.04	1.20	1.44	1.76
m_{3A}	.20	.20	.20	.20	.20
m_{3B}	.86	.88	.89	.91	.93
T_{3A}	3198.00	3198.00	3198.00	3198.00	3198.00
T_{3B}	4693.40	4838.00	4903.40	4849.50	4612.80
T_4	4952.03	5060.26	5105.70	5052.66	4811.14
M_{3B}	2.06	2.05	2.05	2.05	2.04
M_4	1.69	1.71	1.72	1.73	1.73
t_{3B}	2928.40	3010.20	3034.30	2963.10	2753.00
t_4	3614.14	3673.11	3693.04	3628.42	3435.36
P_0	637.87	637.87	637.87	637.87	637.87
P_{2A}	281.96	281.96	281.96	281.96	281.96
P_{2B}	146.73	146.73	146.73	146.73	146.73
P_{3A}	281.96	281.96	281.96	281.96	281.96
P_{3B}	137.56	136.92	136.35	135.71	135.16
P_4	112.21	113.15	113.84	114.66	115.48
p_0	.40	.40	.40	.40	.40
p_{3A}	16.40	16.40	16.40	16.40	16.40
p_{3B}	16.40	16.40	16.40	16.40	16.40
p_4	24.16	23.73	23.46	23.27	23.36
u_{3A}	4666.61	4666.61	4666.61	4666.61	4666.61
u_{3B}	5323.47	5450.17	5539.40	5594.10	5562.50
u_4	4775.56	4894.66	4976.88	5033.38	5011.57
u_e	7454.65	7593.05	7682.08	7717.50	7606.55
u_0	5805.80	5805.80	5805.80	5805.80	5805.80
F	66.22	73.56	79.35	84.77	86.51
S	9.7560e-4	1.0373e-3	1.1102e-3	1.2469e-3	1.4934e-3

Remarks:

1) $M_0 = 6.0$; h = 80,000 ft
2) $\eta_{\Delta T} = 0.6$

TABLE 13

PROPERTIES THROUGH DMRJ (80/20)

Φ_{SFRJ}	1.10	1.30	1.50	1.80	2.20
Φ_{TOT}	.88	1.04	1.20	1.44	1.76
m_{3A}	.20	.20	.20	.20	.20
m_{3B}	.86	.88	.89	.91	.93
T_{3A}	3198.00	3198.00	3198.00	3198.00	3198.00
T_{3B}	4693.40	4838.00	4903.40	4849.50	4612.80
T_4	4871.13	4982.67	5030.63	4979.82	4745.50
M_{3B}	2.06	2.05	2.05	2.05	2.04
M_4	1.74	1.76	1.77	1.77	1.77
t_{3B}	2928.40	3010.20	3034.30	2963.10	2753.00
t_4	3501.87	3565.87	3588.53	3527.28	3344.93
P_0	637.87	637.87	637.87	637.87	637.87
P_{2A}	281.96	281.96	281.96	281.96	281.96
P_{2B}	146.73	146.73	146.73	146.73	146.73
P_{3A}	281.96	281.96	281.96	281.96	281.96
P_{3B}	137.56	136.92	136.35	135.71	135.16
P_4	115.68	116.47	117.16	117.93	118.50
p_0	.40	.40	.40	.40	.40
p_{3A}	16.40	16.40	16.40	16.40	16.40
p_{3B}	16.40	16.40	16.40	16.40	16.40
p_4	23.14	22.79	22.57	22.40	22.54
u_{3A}	4666.61	4666.61	4666.61	4666.61	4666.61
u_{3B}	5323.47	5450.17	5539.40	5594.10	5562.50
u_4	4831.23	4946.70	5028.47	5083.15	5056.53
u_e	7403.50	7544.30	7635.10	7671.05	7562.83
u_0	5805.80	5805.80	5805.80	5805.80	5805.80
F	64.52	71.93	77.76	83.18	84.98
S	1.0012e-3	1.0608e-3	1.1329e-3	1.2708e-3	1.5204e-3

Remarks:

1) $M_0 = 6.0$; h = 80,000 ft
2) $\eta_{\Delta T} = 0.5$

TABLE 14

PROPERTIES THROUGH DMRJ (80/20)

Φ_{SFRJ}	1.10	1.30	1.50	1.80	2.20
Φ_{TOT}	.88	1.04	1.20	1.44	1.76
m_{3A}	.20	.20	.20	.20	.20
m_{3B}	.86	.88	.89	.91	.93
T_{3A}	3198.00	3198.00	3198.00	3198.00	3198.00
T_{3B}	4693.40	4838.00	4903.40	4849.50	4612.80
T_4	4668.90	4788.71	4842.95	4797.74	4581.75
M_{3B}	2.06	2.05	2.05	2.05	2.04
M_4	1.86	1.87	1.88	1.88	1.88
t_{3B}	2928.40	3010.20	3034.30	2963.10	2753.00
t_4	3223.91	3300.05	3331.88	3277.16	3118.25
P_0	637.87	637.87	637.87	637.87	637.87
P_{2A}	281.96	281.96	281.96	281.96	281.96
P_{2B}	146.73	146.73	146.73	146.73	146.73
P_{3A}	281.96	281.96	281.96	281.96	281.96
P_{3B}	137.56	136.92	136.35	135.71	135.16
P_4	126.18	126.41	126.77	127.55	127.62
p_0	.40	.40	.40	.40	.40
p_{3A}	16.40	16.40	16.40	16.40	16.40
p_{3B}	16.40	16.40	16.40	16.40	16.40
p_4	20.74	20.58	20.47	20.34	20.55
u_{3A}	4666.61	4666.61	4666.61	4666.61	4666.61
u_{3B}	5323.47	5450.17	5539.40	5594.10	5562.50
u_4	4963.02	5070.58	5147.29	5200.83	5168.88
u_e	7275.70	7422.45	7517.00	7554.90	7454.49
u_0	5805.80	5805.80	5805.80	5805.80	5805.80
F	60.29	67.85	73.77	79.18	81.18
S	1.0714e-3	1.1246e-3	1.1943e-3	1.3349e-3	1.5916e-3

Remarks:

1) $M_0 = 6.0$; h = 80,000 ft
2) $\eta_{\Delta T} = 0.25$

TABLE 15

PROPERTIES THROUGH DMRJ (80/20)

Φ_{SFRJ}	1.20	1.50	1.80	2.00	2.20
Φ_{TOT}	.96	1.20	1.44	1.60	1.76
m_{3A}	.20	.20	.20	.20	.20
m_{3B}	.87	.89	.91	.92	.93
T_{3A}	1638.00	1638.00	1638.00	1638.00	1638.00
T_{3B}	3837.10	3882.50	3813.00	3728.00	3620.60
T_4	4540.29	4602.13	4394.83	4215.56	4027.05
M_{3B}	2.26	2.25	2.25	2.25	2.25
M_4	1.32	1.33	1.41	1.47	1.53
t_{3B}	2236.70	2222.40	2140.00	2065.10	1979.60
t_4	3718.25	3754.16	3481.94	3262.25	3051.32
P_0	61.34	61.34	61.34	61.34	61.34
P_{2A}	41.77	41.77	41.77	41.77	41.77
P_{2B}	31.95	31.95	31.95	31.95	31.95
P_{3A}	41.77	41.77	41.77	41.77	41.77
P_{3B}	28.76	28.42	28.18	28.05	27.95
P_4	15.94	16.05	16.61	17.09	17.56
p_0	.40	.40	.40	.40	.40
p_{3A}	2.44	2.44	2.44	2.44	2.44
p_{3B}	2.44	2.44	2.44	2.44	2.44
p_4	5.93	5.89	5.43	5.10	4.85
u_{3A}	3316.50	3316.50	3316.50	3316.50	3316.50
u_{3B}	5080.44	5193.07	5222.49	5216.18	5189.83
u_4	3744.51	3837.09	4002.05	4100.34	4160.59
u_e	6297.70	6405.80	6359.22	6284.75	6205.44
u_0	3870.55	3870.55	3870.55	3870.55	3870.55
F	89.24	96.34	98.24	97.97	97.49
S	7.9002e-4	9.1448e-4	1.0759e-3	1.1983e-3	1.3253e-3

Remarks:

1) $M_0 = 4.0$; h = 80,000 ft

2) $\eta_{\Delta T} = 0.9$

TABLE 16

PROPERTIES THROUGH DMRJ (80/20)

Φ_{SFRJ}	1.20	1.50	1.80	2.00	2.20
Φ_{TOT}	.96	1.20	1.44	1.60	1.76
m_{3A}	.20	.20	.20	.20	.20
m_{3B}	.87	.89	.91	.92	.93
T_{3A}	1638.00	1638.00	1638.00	1638.00	1638.00
T_{3B}	3837.10	3882.50	3813.00	3728.00	3620.60
T_4	4197.95	4254.53	4098.51	3956.26	3801.00
M_{3B}	2.26	2.25	2.25	2.25	2.25
M_4	1.56	1.57	1.62	1.66	1.70
t_{3B}	2236.70	2222.40	2140.00	2065.10	1979.60
t_4	3206.91	3236.18	3046.01	2884.58	2723.74
P_0	61.34	61.34	61.34	61.34	61.34
P_{2A}	41.77	41.77	41.77	41.77	41.77
P_{2B}	31.95	31.95	31.95	31.95	31.95
P_{3A}	41.77	41.77	41.77	41.77	41.77
P_{3B}	28.76	28.42	28.18	28.05	27.95
P_4	17.67	17.81	18.40	18.87	19.33
p_0	.40	.40	.40	.40	.40
p_{3A}	2.44	2.44	2.44	2.44	2.44
p_{3B}	2.44	2.44	2.44	2.44	2.44
p_4	4.66	4.63	4.42	4.25	4.12
u_{3A}	3316.50	3316.50	3316.50	3316.50	3316.50
u_{3B}	5080.44	5193.07	5222.49	5216.18	5189.83
u_4	4111.46	4204.95	4297.20	4347.46	4371.70
u_e	6110.30	6214.80	6194.14	6138.50	6075.57
u_0	3870.55	3870.55	3870.55	3870.55	3870.55
F	83.00	89.88	92.57	92.89	92.93
S	8.4937e-4	9.8020e-4	1.1419e-3	1.2639e-3	1.3903e-3

Remarks:

1) $M_0 = 4.0$; h = 80,000 ft
2) $\eta_{\Delta T} = 0.6$

TABLE 17

PROPERTIES THROUGH DMRJ (75/25)

Φ_{SFRJ}	1.10	1.30	1.50	1.80	2.20
Φ_{TOT}	.825	.975	1.125	1.35	1.65
m_{3A}	.25	.25	.25	.25	.25
m_{3B}	.81	.82	.83	.85	.87
T_{3A}	3198.00	3198.00	3198.00	3198.00	3198.00
T_{3B}	4693.40	4838.00	4903.40	4849.50	4612.80
T_4	5144.86	5257.99	5315.18	5300.77	5101.19
M_{3B}	2.06	2.05	2.05	2.05	2.04
M_4	1.55	1.56	1.57	1.55	1.55
t_{3B}	2928.80	3010.60	3034.90	2963.70	2767.00
t_4	3930.61	4000.49	4034.09	4035.50	3864.15
P_0	637.87	637.87	637.87	637.87	637.87
P_{2A}	281.96	281.96	281.96	281.96	281.96
P_{2B}	146.74	146.74	146.74	146.74	146.74
P_{3A}	281.96	281.96	281.96	281.96	281.96
P_{3B}	137.48	136.83	136.25	135.58	135.02
P_4	104.58	105.17	105.50	104.63	104.93
p_0	.40	.40	.40	.40	.40
p_{3A}	16.40	16.40	16.40	16.40	16.40
p_{3B}	16.40	16.40	16.40	16.40	16.40
p_4	28.20	27.74	27.50	27.91	28.04
u_{3A}	4666.61	4666.61	4666.61	4666.61	4666.61
u_{3B}	5322.90	5449.47	5538.60	5593.17	5567.56
u_4	4536.71	4647.34	4722.08	4733.79	4721.40
u_e	7552.75	7696.37	7793.20	7849.98	7826.360
u_0	5805.80	5805.80	5805.80	5805.80	5805.80
F	68.52	75.89	81.78	87.71	92.26
S	8.8438e-4	9.4349e-4	1.0101e-3	1.1298e-3	1.3126e-3

Remarks:

1) $M_0 = 6.0$; h = 80,000 ft
2) $\eta_{\Delta T} = 0.9$

TABLE 18

PROPERTIES THROUGH DMRJ (60/40)

Φ_{SFRJ}	1.30	1.50	1.80	2.20	2.30
Φ_{TOT}	.78	.90	1.08	1.32	1.38
m_{3A}	.40	.40	.40	.40	.40
m_{3B}	.66	.67	.68	.70	.70
T_{3A}	3198.00	3198.00	3198.00	3198.00	3198.00
T_{3B}	4838.00	4903.40	4849.50	4612.80	4534.30
T_4	5095.59	5199.88	5281.00	5271.89	5249.18
M_{3B}	2.05	2.05	2.05	2.04	2.04
M_4	1.52	1.51	1.46	1.37	1.35
t_{3B}	3010.20	3034.30	2963.10	2766.30	2706.50
t_4	3917.36	4024.09	4414.48	4239.85	4240.61
P_0	637.87	637.87	637.87	637.87	637.87
P_{2A}	281.96	281.96	281.96	281.96	281.96
P_{2B}	146.74	146.74	146.74	146.74	146.74
P_{3A}	281.96	281.96	281.96	281.96	281.96
P_{3B}	136.92	136.35	135.71	135.16	135.08
P_4	108.15	106.97	104.78	101.54	100.88
p_0	.40	.40	.40	.40	.40
p_{3A}	16.40	16.40	16.40	16.40	16.40
p_{3B}	16.40	16.40	16.40	16.40	16.40
p_4	30.12	30.65	32.14	35.21	35.98
u_{3A}	4666.61	4666.61	4666.61	4666.61	4666.61
u_{3B}	5450.16	5539.41	5594.11	5568.60	5548.52
u_4	4458.84	4480.46	4438.38	4274.51	4227.20
u_e	7518.44	7634.66	7742.18	7800.58	7815.95
u_0	5805.80	5805.80	5805.80	5805.80	5805.80
F	66.62	72.53	79.27	85.52	87.09
S	8.6010e-4	9.1137e-4	1.0004e-3	1.1343e-3	1.1632e-3

Remarks:

1) $M_0 = 6.0$; h = 80,000 ft
2) $\eta_{\Delta T} = 0.9$

TABLE 19

PROPERTIES THROUGH DMRJ (50/50)

Φ_{SFRJ}	1.20	1.50	1.80	2.00	2.20
Φ_{TOT}	.60	.75	.90	1.00	1.10
m_{3A}	.50	.50	.50	.50	.50
m_{3B}	.54	.56	.57	.57	.58
T_{3A}	3198.00	3198.00	3198.00	3198.00	3198.00
T_{3B}	4923.00	5007.70	4906.30	4785.70	4638.40
T_4	4959.27	5206.12	5364.06	5425.81	5454.29
M_{3B}	2.44	2.44	2.44	2.44	2.44
M_4	1.74	1.66	1.57	1.51	1.45
t_{3B}	2737.00	2749.70	2642.50	2544.80	2435.30
t_4	3558.25	3849.85	4087.70	4202.44	4307.33
P_0	637.87	637.87	637.87	637.87	637.87
P_{2A}	637.87	637.87	637.87	637.87	637.87
P_{2B}	637.87	637.87	637.87	637.87	637.87
P_{3A}	637.87	637.87	637.87	637.87	637.87
P_{3B}	596.23	592.67	590.18	588.97	588.06
P_4	343.50	327.83	312.65	303.03	297.10
p_0	.40	.40	.40	.40	.40
p_{3A}	37.08	37.08	37.08	37.08	37.08
p_{3B}	37.08	37.08	37.08	37.08	37.08
p_4	69.08	74.57	81.74	85.83	92.62
u_{3A}	4666.61	4666.61	4666.61	4666.61	4666.61
u_{3B}	6072.34	6215.17	6248.42	6234.66	6198.93
u_4	4813.48	4784.97	4677.20	4596.10	4470.48
u_e	7760.03	8000.26	8153.93	8236.10	8276.85
u_0	5805.80	5805.80	5805.80	5805.80	5805.80
F	71.38	81.91	89.73	94.33	97.56
S	6.1786e-4	6.7271e-4	7.3662e-4	7.7816e-4	8.2716e-4

Remarks:

1) $M_0 = 6.0$; h = 80,000 ft
2) $\eta_{\Delta T} = 0.9$
3) Isentropic inlet

INITIAL DISTRIBUTION LIST

		No. Copies
1.	Defense Technical Information Center Cameron Station Alexandria, Virginia 22304-6145	2
2.	Naval Weapons Center China Lake, California 93555-6001 F. Zarlingo, Code 32403	2
3.	Library, Code 0142 Naval Postgraduate School Monterey, California 93943-5002	2
4.	Department Chairman Department of Aeronautics, Code 67 Naval Postgraduate School Monterey, California 93943-5026	1
5.	Prof. David W. Netzer Department of Aeronautics, Code 67Nt Naval Postgraduate School Monterey, California 93943-5004	3
6.	Prof. Ray Shreeve Department of Aeronautics, Code 67Sf Naval Postgraduate School Monterey, California 93943-5004	1
7.	Dr. Alon Gany Department of Aeronautical Engineering Technion, Haifa 32000, Israel	2
8.	Lt. Clifford B. Vaught Operations Department USS Independence (CV - 62) FPO New York, N.Y. 09537-2760	5
9.	Mrs. Herta Vaught 104 South Kelly Avenue, Apt. 5 Bel Air, Maryland 21014	1

Thesis
V355
c.1

Vaught
An investigation into the feasibility of using a dual-combustion mode ramjet in a high Mach number tactical missile.